



**University of  
Zurich**<sup>UZH</sup>

**Zurich Open Repository and  
Archive**

University of Zurich  
University Library  
Strickhofstrasse 39  
CH-8057 Zurich  
[www.zora.uzh.ch](http://www.zora.uzh.ch)

---

Year: 2019

---

## Postoperative Spinal CT: What the Radiologist Needs to Know

Ghudasara, Nevil ; Yi, Paul H ; Clark, Karen ; Fishman, Elliot K ; Farshad, Mazda ; Fritz, Jan

**Abstract:** During the past 2 decades, the number of spinal surgeries performed annually has been steadily increasing, and these procedures are being accompanied by a growing number of postoperative imaging studies to interpret. CT is accurate for identifying the location and integrity of implants, assessing the success of decompression and intervertebral arthrodesis procedures, and detecting and characterizing related complications. Although postoperative spinal CT is often limited owing to artifacts caused by metallic implants, parameter optimization and advanced metal artifact reduction techniques, including iterative reconstruction and monoenergetic extrapolation methods, can be used to reduce metal artifact severity and improve image quality substantially. Commonly used and recently available spinal implants and prostheses include screws and wires, static and extendable rods, bone grafts and biologic materials, interbody cages, and intervertebral disk prostheses. CT assessment and the spectrum of complications that can occur after spinal surgery and intervertebral arthroplasty include those related to the position and integrity of implants and prostheses, adjacent segment degeneration, collections, fistulas, pseudomeningoceles, cerebrospinal fluid leaks, and surgical site infections. Knowledge of the numerous spinal surgery techniques and devices aids in differentiating expected postoperative findings from complications. The various types of spinal surgery instrumentation and commonly used spinal implants are reviewed. The authors also describe and illustrate normal postoperative spine findings, signs of successful surgery, and the broad spectrum of postoperative complications that can aid radiologists in generating reports that address issues that the surgeon needs to know for optimal patient management. ©RSNA, 2019.

DOI: <https://doi.org/10.1148/rg.2019190050>

Posted at the Zurich Open Repository and Archive, University of Zurich

ZORA URL: <https://doi.org/10.5167/uzh-177275>

Journal Article

Published Version



The following work is licensed under a Creative Commons: Attribution-NonCommercial 4.0 International (CC BY-NC 4.0) License.

Originally published at:

Ghudasara, Nevil; Yi, Paul H; Clark, Karen; Fishman, Elliot K; Farshad, Mazda; Fritz, Jan (2019). Postoperative Spinal CT: What the Radiologist Needs to Know. *Radiographics*, 39(6):1840-1861.

DOI: <https://doi.org/10.1148/rg.2019190050>



# Postoperative Spinal CT: What the Radiologist Needs to Know

Nevil Ghodasara, MD  
Paul H. Yi, MD  
Karen Clark, MD  
Elliot K. Fishman, MD  
Mazda Farshad, MD, MPH  
Jan Fritz, MD

**Abbreviations:** ACDF = anterior cervical discectomy and fusion, BMP = bone morphogenetic protein

**RadioGraphics 2019;** 39:1840–1861

<https://doi.org/10.1148/rg.2019190050>

**Content Codes:** **CT** **ER** **HN** **NR**

From the Russell H. Morgan Department of Radiology and Radiologic Science (N.G., P.H.Y., K.C.), Sections of Body CT (E.K.F.) and Musculoskeletal Radiology (J.F.), Johns Hopkins Hospital, 601 N Caroline St, Room 3014, Baltimore, MD 21287; and Spine Division, Department of Orthopedics, Balgrist University Hospital Zurich, Zurich, Switzerland (M.F.). Presented as an education exhibit at the 2018 RSNA Annual Meeting. Received March 8, 2019; revision requested May 8 and received June 21; accepted June 26. For this journal-based SA-CME activity, the authors E.K.F., M.F., and J.F. have provided disclosures (see end of article); all other authors, the editor, and the reviewers have disclosed no relevant relationships. **Address correspondence to** J.F. (e-mail: [jfritz9@jhmi.edu](mailto:jfritz9@jhmi.edu)).

©RSNA, 2019

## SA-CME LEARNING OBJECTIVES

*After completing this journal-based SA-CME activity, participants will be able to:*

- Describe the technical challenges, and related solutions, of performing postoperative spinal CT in patients with metal implants.
- List the different categories of spinal surgery and the various instrumentations and implants used in spinal procedures.
- Identify normal and abnormal findings at postoperative spinal CT.

*See [rsna.org/learning-center-rg](http://rsna.org/learning-center-rg).*

During the past 2 decades, the number of spinal surgeries performed annually has been steadily increasing, and these procedures are being accompanied by a growing number of postoperative imaging studies to interpret. CT is accurate for identifying the location and integrity of implants, assessing the success of decompression and intervertebral arthrodesis procedures, and detecting and characterizing related complications. Although postoperative spinal CT is often limited owing to artifacts caused by metallic implants, parameter optimization and advanced metal artifact reduction techniques, including iterative reconstruction and monoenergetic extrapolation methods, can be used to reduce metal artifact severity and improve image quality substantially. Commonly used and recently available spinal implants and prostheses include screws and wires, static and extendable rods, bone grafts and biologic materials, interbody cages, and intervertebral disk prostheses. CT assessment and the spectrum of complications that can occur after spinal surgery and intervertebral arthroplasty include those related to the position and integrity of implants and prostheses, adjacent segment degeneration, collections, fistulas, pseudomeningoceles, cerebrospinal fluid leaks, and surgical site infections. Knowledge of the numerous spinal surgery techniques and devices aids in differentiating expected postoperative findings from complications. The various types of spinal surgery instrumentation and commonly used spinal implants are reviewed. The authors also describe and illustrate normal postoperative spine findings, signs of successful surgery, and the broad spectrum of postoperative complications that can aid radiologists in generating reports that address issues that the surgeon needs to know for optimal patient management.

©RSNA, 2019 • [radiographics.rsna.org](http://radiographics.rsna.org)

## Introduction

Owing to innovations in surgical techniques and devices, the frequencies of spinal surgery procedures have been increasing steadily during the past decades. Between the years 2004 and 2015, the number of elective spinal surgeries performed to achieve lumbar fusion reportedly increased from 122 679 to 199 140 (1). This amounted to a 177% increase in total hospital costs, with more than \$10 billion in hospital costs in 2015 (1). Similarly, the total number of cervical spine surgeries performed reportedly increased from 27 061 to 34 582 between the years 2001 and 2013, with a 64% increase in costs (2). The highest rate of increase in the volume of spinal surgery procedures occurred among individuals aged 65 years or older (1). With a prevalence of 23% (3), neck pain and lower back pain are the two main indications for spinal surgery, and the prevalence is likely to increase owing to the growing population of elderly persons.

## TEACHING POINTS

- An interbody graft is accurately positioned when the distance between the radiopaque marker of the posterior graft margin and the posterior vertebral body margin is 2 mm or greater. When the interbody graft is placed closer than 2 mm to the posterior margin of the endplate, there is an increased risk of posterior migration into the spinal canal, with mass effect on the ventral thecal sac.
- The clinical importance of variant implant positioning is usually unknown. Screws may breach the osseous cortex and even come in contact with the thecal sac, neural elements, or paraspinal structures, causing symptoms or adverse clinical outcomes. Although pedicle screw breaches have been reported in up to 5.1% of cases, neurologic symptoms occur with a frequency of less than 0.2%.
- Circumferential peri-implant osteolysis around spinal implants larger than 2 mm suggests implant loosening. However, to diagnose implant loosening with certainty, a change in the position of the implant must be demonstrated at serial imaging.
- The pattern of peri-implant osteolysis can help differentiate an infectious cause from a mechanical loosening-related cause. With mechanical loosening of a screw, the osteolysis may be more prominent along the distal tip owing to a pivot point around which the screw moves, whereas infectious osteolysis is often more diffuse.
- Adjacent segment disease is the development or progression of motion segment degeneration directly above and below a spinal instrumentation construct. In adjacent segment disease, the degeneration is accelerated secondarily to the summation of forces and resultant increased transmission of the biomechanical load from the instrumentation-managed and immobilized spinal segments. These segments act as a lever arm and exert torque forces at the levels of the adjacent native motion segments above and below the instrumentation construct.

The increasing numbers of spinal surgeries are resulting in increasing numbers of postoperative imaging studies for radiologists to interpret. Knowledge of the initial clinical manifestations and imaging characteristics of the preoperative spinal abnormality (or abnormalities), type of surgery performed, and length of time since surgery is helpful for accurately interpreting a postoperative spinal imaging study. This knowledge is also helpful for subsequent patient management. In addition, having an understanding of spinal surgery techniques, approaches, and devices aids in differentiating expected postoperative findings from abnormalities and complications.

CT is accurate for identifying the location and integrity of implants, assessing the success of decompression and intervertebral arthrodesis, and detecting and characterizing complications. Used in conjunction with radiography, CT is a powerful problem-solving tool for detecting radiographically occult abnormalities and characterizing suspected abnormalities.

In this article, we review various types of spinal surgery procedures and describe commonly used

spinal implants. We further describe and illustrate normal postoperative findings, signs of successful surgery, and a wide spectrum of common and less common postoperative complications, which can aid radiologists in generating reports that address issues that the surgeon needs to know for optimal patient management.

## Imaging Modalities

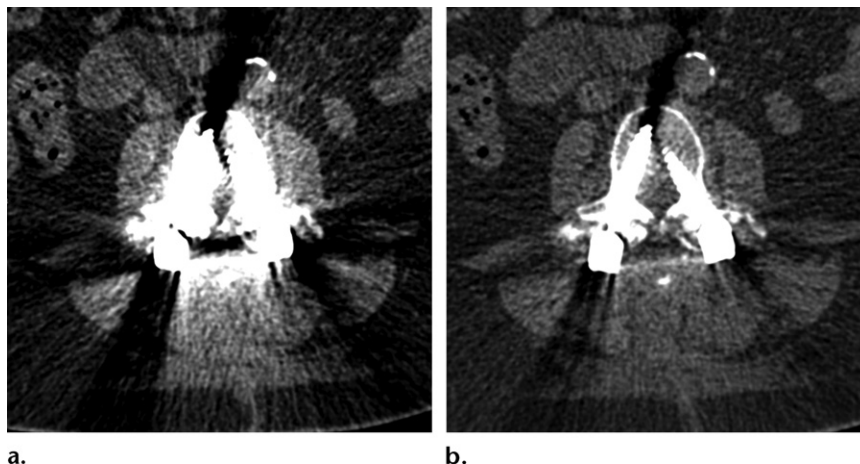
Radiography is the primary modality used for immediate postoperative assessment and long-term follow-up after spinal instrumentation surgery. Although radiography has limitations, it often can be used to determine the position of the implant and progression of osseous fusion, and to diagnose with certainty complications such as fractures and adjacent segment degeneration (4). A comparison of follow-up radiographic findings to baseline postoperative radiographic findings is important for detecting changes in device position and loss of implant fixation. US can be used to detect and characterize superficially located collections; however, accurate characterization of the depth of involvement is often difficult or not possible with this modality.

Radionuclide imaging, including technetium 99m medronate bone scintigraphy, can be used to diagnose osteomyelitis. However, the high sensitivity of this modality often interferes with identification of the specific underlying abnormality. Gallium 67 scintigraphy has higher specificity than does triple-phase bone scanning. Thus, these two examinations are often combined (5). Labeled leukocyte scintigraphy and fluorine 18 fluorodeoxyglucose PET/CT may be used to successfully diagnose spinal infection.

In the postoperative setting, MRI is used primarily to visualize spinal canal patency and nerve root compression, and, importantly, to detect and characterize collections and infections (6). However, artifacts from metallic implants may limit the usefulness of MRI in their immediate vicinity.

After spinal instrumentation surgery, common indications for CT include characterization of the integrity and position of the implant, visualization of the presence and progression of osseous fusion, and diagnosis of complications such as peri-implant osteolysis, radiographically occult fractures, and soft-tissue collections (4). CT depicts osseous structures with high detail, and high-spatial-resolution isotropic datasets enable capability for multiplanar reformations, which can improve the evaluation of implant position and alignment, and osseous fusion. Ultimately, multiplanar reformation capability facilitates improved assessment of the success of the surgery. CT myelography is an invasive examination that serves as an alternative to MRI in evaluations of

**Figure 1.** Metal artifact reduction at CT of a 62-year-old woman who underwent posterior spinal instrumentation surgery at the L3–S1 vertebral body level with pedicle screws, vertical rods, midline decompression, and posterolateral bone graft placement. Axial CT images at the level of the L3 vertebral body at 100 keV (a) and 140 keV (b) show increased metal artifact severity and contrast resolution at 100 keV, with decreased metal artifact severity and contrast resolution at 140 keV.



the spinal canal and nerve roots when infection, fibrosis, or impingement is suspected. Furthermore, it can be used to determine the location of postoperative cerebrospinal fluid leaks (4).

### CT Techniques and Protocols

In the presence of metallic implants, CT evaluation of the spine is limited by implant-related artifacts. When the x-ray beam traverses high-attenuation implants, photon starvation, beam hardening, and beam scattering occur and manifest as dark and bright bandlike or streaklike artifacts on CT images. These artifacts limit the visibility of the implant and surrounding structures (7). The severity of artifacts depends on fixed and modifiable variables. Fixed variables are based on the inherent properties of the implant, including the composition and geometric features of the metal. The higher the density of the metal, the more artifacts will be produced (8). Hence, titanium, which is less dense than stainless steel, causes less x-ray attenuation and fewer artifacts (9). Polyetheretherketone is a material commonly used for interbody grafts and has many useful properties, including the feature that it causes minimal artifacts on CT images (4). The thicker the implant, the higher the attenuation and the greater the artifact severity.

Improvement of the image quality and diagnostic accuracy of postoperative spinal CT is mainly dependent on the modifiable variables, which are related to the CT techniques, parameters, and protocols used. Several modifiable variables can be optimized to improve CT image quality in the presence of spinal implants. Performing imaging perpendicular to the implant, with the x-ray beam traversing the smallest cross section, reduces the severity of artifacts (10).

Image acquisition factors that reduce artifact severity include high peak voltage, high tube current, narrow collimation, and thin sections (11). The peak voltage (Fig 1) affects the ability of an

x-ray beam to penetrate a structure, and the tube current corresponds to the number of photons that reach the detectors to produce the CT image. Use of a higher peak voltage and higher tube current results in fewer artifacts (10). However, the quadratic relationship between increasing peak voltage and increasing radiation dose should be carefully considered. In addition, the use of higher peak voltages leads to decreased contrast resolution on CT images, which can interfere with the detectability of soft-tissue processes.

Patient motion during image acquisition causes additional artifacts but is minimized owing to the high speed of data acquisition achieved with current multidetector CT scanners (9). Acquiring CT data with use of a low pitch can decrease the severity of implant-related artifacts, whereas the use of smooth reconstruction kernels facilitates a decrease in noise. High-spatial-resolution datasets with an isotropic voxel size equal to or less than  $0.75 \times 0.75 \times 0.75 \text{ mm}^3$  yield high image detail and enable three-dimensional postprocessing (12,13).

Metal implant-induced CT artifacts can be further minimized by using advanced techniques, including metal artifact reduction reconstruction algorithms and dual-energy data acquisition with virtual monoenergetic extrapolation postprocessing (14). Although many vendors have their own proprietary reconstruction algorithms and metal artifact reduction software, many use projection completion. With projection completion, inaccurate or missing x-ray projections are replaced by interpolations from adjacent projections (14). Dual-energy CT images can be acquired by using several different methods, most of which involve the use of specialized CT scanner systems (Fig 2) (14,15).

On the basis of the CT datasets acquired with different tube energies, several calculations can be performed to determine the differential mass densities of the base materials. When the differ-



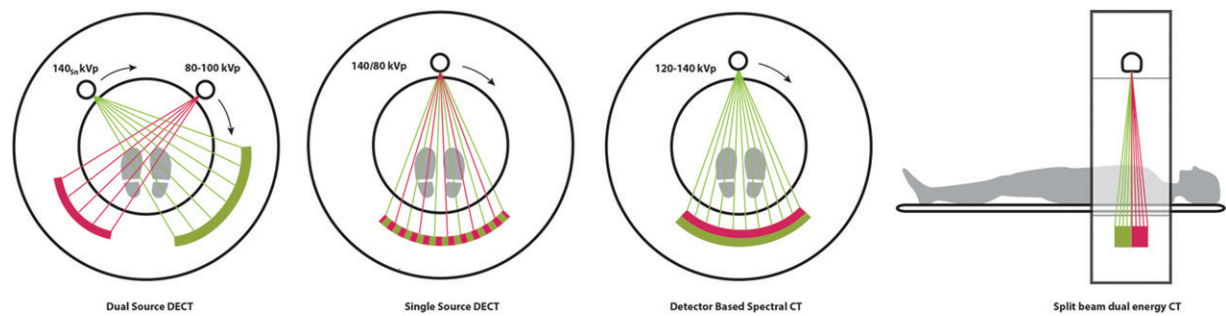


**Figure 2.** Drawings illustrate dual-energy CT (DECT) acquisition techniques, including dual-source dual-energy CT with two x-ray tubes and two detectors (far left), single-source dual-energy CT with fast tube energy switching (second from left), single-source detector-based spectral CT (third from left), and single-source dual-energy CT with split x-ray beam technology (far right).

ential mass densities are combined with the mass attenuation coefficients, virtual monoenergetic images can be created (14). The acquisition of virtual monoenergetic images at higher energies reduces the severity of high-attenuation beam-hardening artifacts (Fig 1), but it does not account for other causes of artifacts such as scattering (16).

Iterative and monoenergetic CT techniques can be used to substantially reduce spine implant- and prosthesis-induced metal artifacts and improve the visibility of bone, soft tissues, and pathologic processes (17–19). The use of three-dimensional postprocessing with multiplanar and curved reformations, as well as volume and cinematic rendering techniques, can further decrease the severity of streak artifacts by averaging the axial data in reformation planes in which true signal and random artifacts are balanced (14,20).

### Spinal Instrumentation Techniques

Familiarity with the indications for a given spinal surgery, types of procedures performed, and goals of the surgical intervention aids in the accurate interpretation of postoperative CT findings. The main types of spinal surgery include decompression, fixation, stabilization and fusion, deformity correction, and lesion excision and débridement (10,15,21–23).

Decompression is mainly performed to minimize mass effects by means of herniated disk material removal or to relieve spinal or neuroforaminal stenosis. Decompression can be achieved by performing a laminotomy, sequestrectomy, or (optional) nucleotomy if the annulus defect is surgically accessible. Unilateral laminotomy involves the removal of a portion of the lamina to gain access for stepwise removal of disk fragments in the setting of a herniated disk (23). Midline laminotomy, which includes the removal of the caudal part of the upper lamina and the cranial part of the lower lamina, is the standard procedure for surgical treatment of spinal stenosis.

Laminectomy involves the complete removal of the lamina, and it can be unilateral, with removal

of one lamina, or bilateral, with removal of both laminae and the spinous process. Rarely, this procedure is used in extensive midline decompression procedures to relieve spinal canal stenosis.

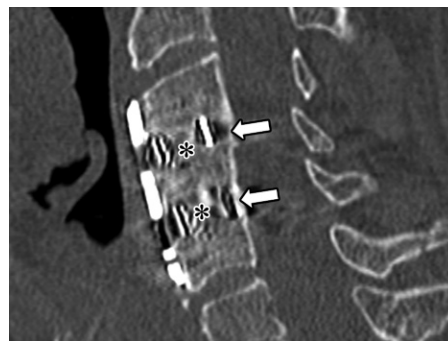
A partial facetectomy is indicated when an exiting nerve root is compressed. The goal is to remove only enough of the facet joint to decompress the nerve root without causing segmental instability, which may result in anterior subluxation (23). Laminectomy and facetectomy are usually accompanied by instrumentation for fixation.

Stabilization is performed to achieve osseous spinal fusion when there is suspected or proven instability as a result of degenerative disk disease, spondylolysis with spondylolisthesis, trauma, infection, and/or malignancy. In this setting, the goals of spinal implants are to (a) immobilize the motion segment to allow osseous fusion, (b) maintain or restore alignment, and (c) enable the ability to adequately address biomechanical forces after the removal of a portion of the spine.

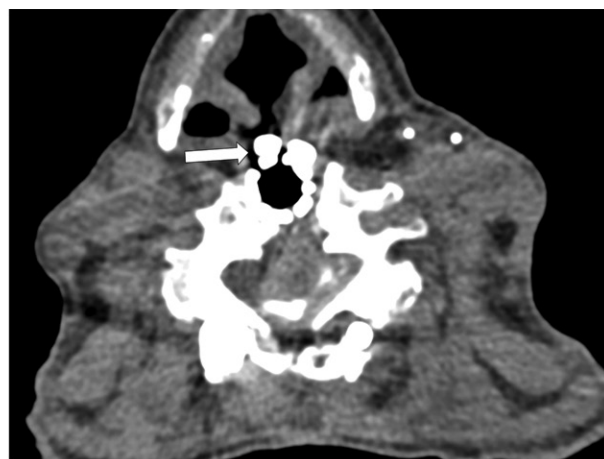
Many published and nonpublished surgical approaches and spinal instrumentation systems are based on the clinical scenario, local expertise, practice preferences, and current abnormalities. In this review, we describe the concepts that are most pertinent for the interpretation of postoperative CT findings.

There are multiple anterior and posterior surgical approaches to the cervical spine, depending on the underlying abnormality and level of involvement (24). The classic approach for the cervical spine is the Smith-Robinson anterior approach, which is used for anterior access to the C2–T1 cervical spine level in several procedures, including anterior cervical discectomy and fusion (ACDF), anterior cervical corpectomy and fusion, and cervical disk replacement. A transoral approach is needed to access the clivus and the C1 and C2 vertebral bodies (25). The posterior approach, which is less preferred, may be performed for laminoplasty, laminectomy, and posterior instrumentation. Posterior cervical spinal instrumentation involves placing lateral

**Figure 3.** ACDF in a 62-year-old woman who underwent cervical spinal instrumentation extending from the C3 to C5 motion segments, including C3–C4 and C4–C5 discectomies with interbody graft placements, and anterior plate and screw fixation. Sagittal CT image shows the vertebral anatomy after successful intervertebral arthrodesis, as indicated by solid osseous bridging through (\*) and around (arrows) the interbody grafts.



**a.**



**b.**

**Figure 4.** Fistula in a 66-year-old woman who underwent posterior cervicthoracic instrumentation including C5–T1 corpectomies with interbody graft placement, C4–T2 anterior plate and screw fixation, and posterior C2–T5 pedicle screw and rod fixation. Sagittal CT image of the cervical spine enhanced with oral iodine-based contrast material (**a**) and axial CT myelography image of the cervical spine (**b**) show a fistula (arrow) between the esophagus and interbody graft. There is mature osseous bridging across the posterolateral bone graft site (arrowheads in **a**).

mass screws in the C3–C7 vertebral bodies and transpedicular screws in the C2 vertebral body with vertical rods bilaterally (24,25). In certain clinical scenarios, a combined anterior and posterior approach may be performed. Advancements in patient-specific instrumentation and navigation techniques enable the placement of pedicle screws in the C3–C6 vertebral bodies (26).

ACDF is the most commonly used technique for the surgical treatment of central and foraminal stenoses (27) (Fig 3). It involves removal of the intervertebral disk (discectomy) and placement of an interbody cage or tricortical bone graft to restore neural foraminal height, maintain the cervical lordosis, and promote intervertebral arthrodesis (4). An anterior plate with unicortical or bicortical screws can be added at multilevel ACDF, in cases of traumatic lesions, and when only a tricortical bone graft, rather than a titanium, polyetheretherketone, or carbon cage, is placed to improve the promotion of osseous fusion. In anterior cervical corpectomy and fusion, one or more vertebral bodies are resected (Fig 4) (10). An interbody

cage with bone graft material is most commonly used to replace the resected vertebral bodies (28). Resection of more than two vertebral bodies often requires additional posterior stabilization.

Disk replacement is performed to maintain physiologic segmental motion in younger patients who do not have degenerative facet or uncovertebral arthrosis (Figs 5, 6) (4). Most implants have a ball-and-socket design, with the superior and inferior base plates of the prosthesis secured to the vertebral body above and below by keels, spikes, or screws. However, the number of different designs is increasing.

There are various basic approaches and techniques for lumbar spinal surgery (Fig 7). However, many variations and individual techniques and approaches exist (9,29). Recognition of the surgical approach used enables the radiologist to predict the sites of surgical dissection changes in both the body wall and the surgical bed. Evaluation of paraspinal anatomic structures such as the psoas muscle and abdominal vasculature is helpful for determining the surgical approach (23,29).

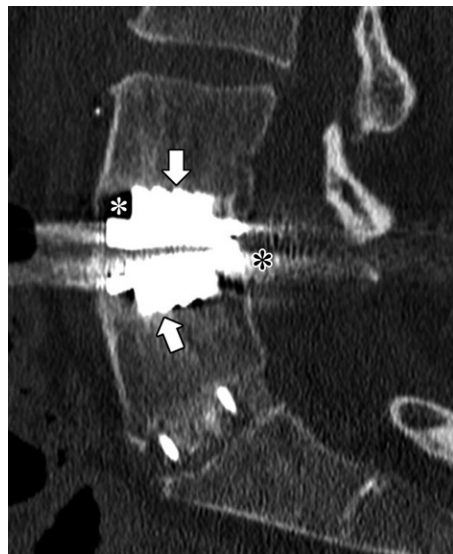


**Figure 5.** Lumbar intervertebral disk replacement in a 48-year-old man who underwent the procedure because of back pain related to disk degeneration of the L4-L5 motion segment. Sagittal CT image shows accurate placement and anchoring of the disk prosthesis within the endplates and successful osseous integration, as indicated by the extension of cancellous bone to the implant surfaces (arrows) without sclerosis or osteolysis. The anatomic alignment of the lumbar spine is preserved. Dark (white \*) and bright (black \*) metal artifacts are seen.

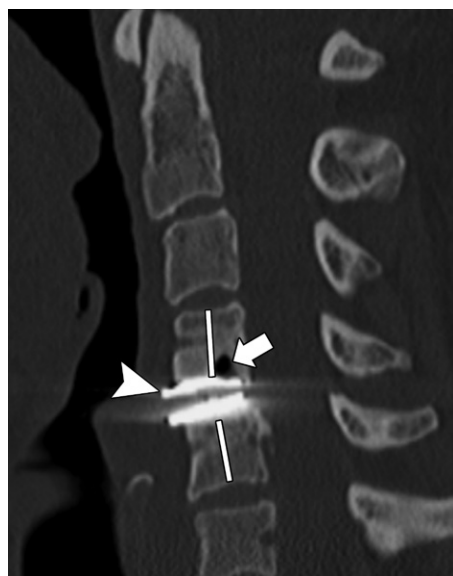


**Figure 6.** Cervical intervertebral disk replacement in a 51-year-old man who underwent the procedure because of back pain related to disk degeneration of the C4-C5 motion segment. Sagittal CT image shows variant placement of the disk prosthesis, with the implant margins (arrowhead) anteriorly positioned approximately 3 mm from the endplates. Consequently, there is nonanatomic alignment with mild posterior angulation of the superior-inferior implant axes, a disproportional anterior opening, and mild segmental lordosis (lines). A small area of subcortical osteolysis (arrow) also is seen.

A posterior approach is most common and enables access to the posterior elements, spinal canal, and disk (23). Laminotomy, laminectomy, facetectomy, and discectomy, along with pedicle screw and rod fixation, may be performed according to the indication for and intent of the surgery (23). Anterior approaches are used primarily to access the lumbosacral junction. Indications for lateral approaches include discectomy with interbody graft placement when there is no need for posterior decompression and when indirect posterior decompression is intended through the following distraction of the posterior elements (29).

## Spinal Instrumentation and Implant Nomenclature

Spinal fixation can be accomplished by using a variety of implants (21,22,30,31). There are many different instrumentation systems, devices, implants, and individualized constructs. We provide an overview of the most commonly used spinal implants and devices that are most relevant in the interpretation of postoperative spinal CT findings.

### Screws and Wires

Screws are used for various purposes in spinal surgery, from fracture fixation to surgery for osseous spinal fusion (Fig 3). Single screws can provide stability and compression for the healing of fractures, such as unilateral pars fracture; however, they are rarely indicated. Pairs of transpedicular, translaminar, and transarticular screws serve as anchors for posterior connecting rods in posterior spinal fixation constructs to achieve osseous spinal fusion and intervertebral arthrodesis (25). Screws are used to fix plates to vertebral osseous elements to provide stability for osseous spinal fusion, such as that in ACDF procedures (21). Although wires placed in the sublaminar position are now used less commonly than screws, they can provide stability for fracture fixation (32) and deformity correction (33).

### Plates

When used together with screws, plates provide stability and induce compression in spinal constructs that are used in the setting of neural decompressions, traumatic injuries, osseous defects, and oncologic reconstructions (Figs 3, 4). Plates are typically placed in an anterior, anterolateral, or lateral position and span two or more vertebral levels. They usually have a low-profile design to be as flush as possible with the vertebral body cortex and to minimize injury or irritation to adjacent structures and organs.

### Rods

Rods are used in conjunction with anchoring pedicle screws to stabilize a fixation construct,



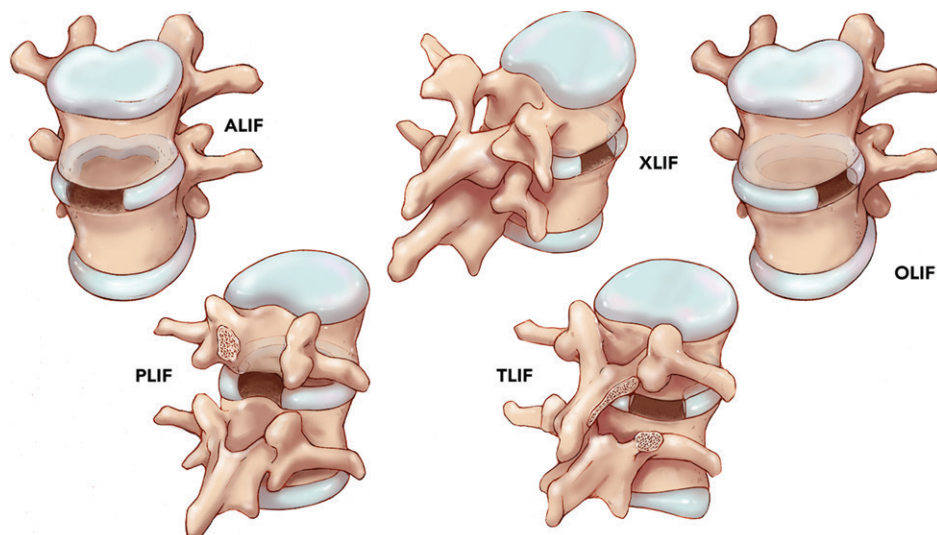


**Figure 7.** Drawings depict several surgical approaches for interbody graft placement in the lumbar spine. Anterior (ALIF), oblique (OLIF), lateral (XLIF), transforaminal (TLIF), and posterior (PLIF) lumbar interbody fusion access techniques, with different discectomy access sites, are illustrated. Anatomic structures, including the psoas muscle and abdominal vasculature, guide the surgical approach at various lumbar levels. Posterior lumbar interbody fusion access involves bilateral laminotomies, with removal of the posterior element. Transforaminal lumbar interbody fusion access involves unilateral laminectomy and inferior facetectomy.

correct deformity, and maintain alignment of the spine through distraction, such as that used in scoliosis correction surgery (Fig 8). Although the eponym *Harrington rod* is frequently used to describe posterior spinal fixation rods, it describes a specific rod that was designed in the early 1960s (34) and used for scoliosis correction surgery until the late 1990s. Similarly, the Luque rod was introduced in the early 1980s (35) as an alternative tool for posterior fixation and distraction involving the use of sublaminar wires to fix rods. However, neither the Harrington rod nor the Luque rod is used in modern spinal surgeries. Given the wide variability of rod designs in modern spinal fixation constructs, the use of simple descriptors such as “rod” can often prevent inaccuracies.

Growing rods (36) are used for adjustable fixation constructs in scoliosis correction surgery (Figs 9, 10). In a growing rod construct, one or two rods are fixed to the screws or hooks above and below the scoliotic curve. The rods include mechanisms that enable incremental lengthening either by means of minimally invasive surgical access or noninvasively by means of transcutaneous application of magnetic forces (eg, with an external remote controller) (37).

The core component of a growing rod construct is the actuator, which is wider than the proximal and distal rod components. The actuator houses the internal magnet and distraction mechanism of the rod. Actuators come in different sizes, which facilitate the capacity for different postoperative distractions. For example, 70- and 90-mm

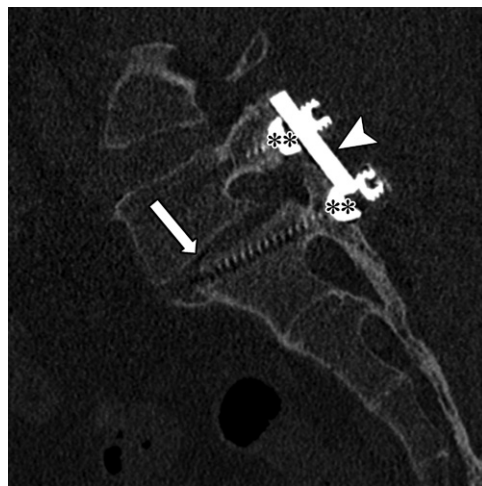


**Figure 8.** Rod disengagement in a 62-year-old man who underwent posterior lumbar spinal instrumentation extending from the L5 to S1 vertebral bodies to address Meyerding grade 1 anterolisthesis. Sagittal CT image shows mechanical rod disengagement characterized by angular malalignment and superior migration of the rod (arrowhead) relative to the connector (\*\*). A small vacuum cleft phenomenon (arrow) in the disk space and the lack of osseous bridging indicate micromotion and construct instability.

actuators can provide a maximum of 28 and 48 mm of postoperative distraction, respectively.

There are two rod polarities: standard rods and offset rods. In the standard rod, the magnet is housed within the distal or inferior portion of the actuator and lengthening occurs in a cephalic direction. In contrast, in the offset rod, the mag-



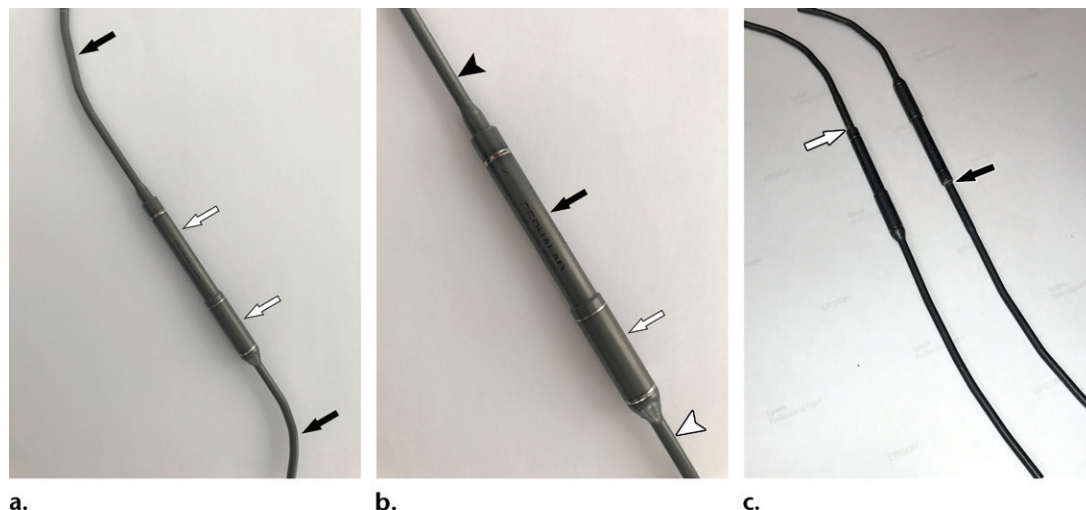


**Figure 9.** Photographs show magnetically controlled growing rods. **(a)** Each rod consists of an actuator component (white arrows), which houses the magnet and lengthening mechanism, and rods (black arrows), which the surgeon adapts to the kyphotic and lordotic spinal curvature. **(b)** In a standard rod, lengthening in the actuator occurs in cephalic directions. The actuator consists of a more narrowed sleeve component (black arrow) and a wider magnet component (white arrow). The rods can be differentiated as the extendable telescopic rod (black arrowhead) and the static rod (white arrowhead). **(c)** A standard rod (white arrow) and offset rod (black arrow) construct allows independent lengthening with use of an external remote controller (not shown).

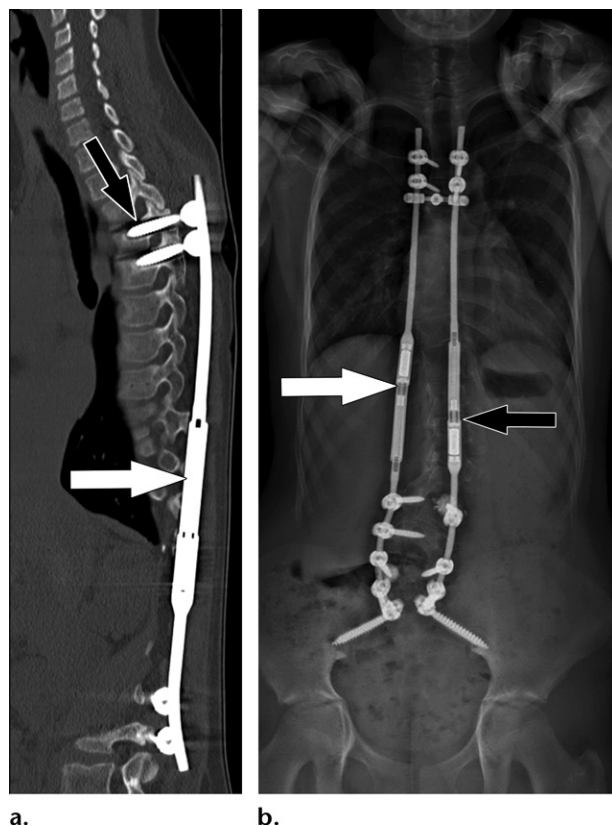


**Figure 10.** Scoliosis correction with magnetically controlled growing rods in a 7-year-old girl with Marfan syndrome. **(a)** Sagittal CT image of a unilateral standard growing rod shows the actuator with a lengthening mechanism (white arrow) in the cephalic direction, and the rods. The osteolysis (black arrow) around the proximal anchoring screws indicates unsuccessful osseous fixation. **(b)** Frontal radiograph of the spine after revision surgery shows a construct consisting of a standard rod (black arrow) and offset rod (white arrow). This construct allows independent lengthening in caudal (offset rod) and cephalic (standard rod) directions with use of an external remote controller (not shown).

net is housed in the proximal or superior portion of the actuator and lengthening occurs in a caudal direction (Figs 9, 10). In a construct with two standard rods, the rods can be lengthened simultaneously, whereas a construct with standard and offset rods enables independent lengthening when an external remote controller is used.

### Bone Grafts and Other Biologic Materials

Bone grafts are often used posterolaterally in fixation constructs as biologic adjuncts to promote osseous fusion. Bone grafts are autologous when they are harvested from the patient and allogenic when they are harvested from cadaveric bone. Other biologic materials used to promote osseous fusion include demineralized bone matrix and bone morphogenetic protein (BMP) (38). On CT images, these materials often have the appearance of osseous elements at the instrumentation sites.

### Interbody Cages

Interbody grafts and cages, which may also be referred to as intervertebral spacers, have varying designs and are commonly used to restore disk height after discectomy and promote immobilizing osseous bridging across the disk space (Fig 3). Solid interbody cages usually are hollow and thus can be packed with other biologic materials (7,25). Interbody grafts may be composed of metallic alloys such as titanium; plastics such as polyetheretherketone; carbon fibers; and ceramics. Some cages are designed to not only restore disk height but also replace an entire vertebral body or segment of vertebral

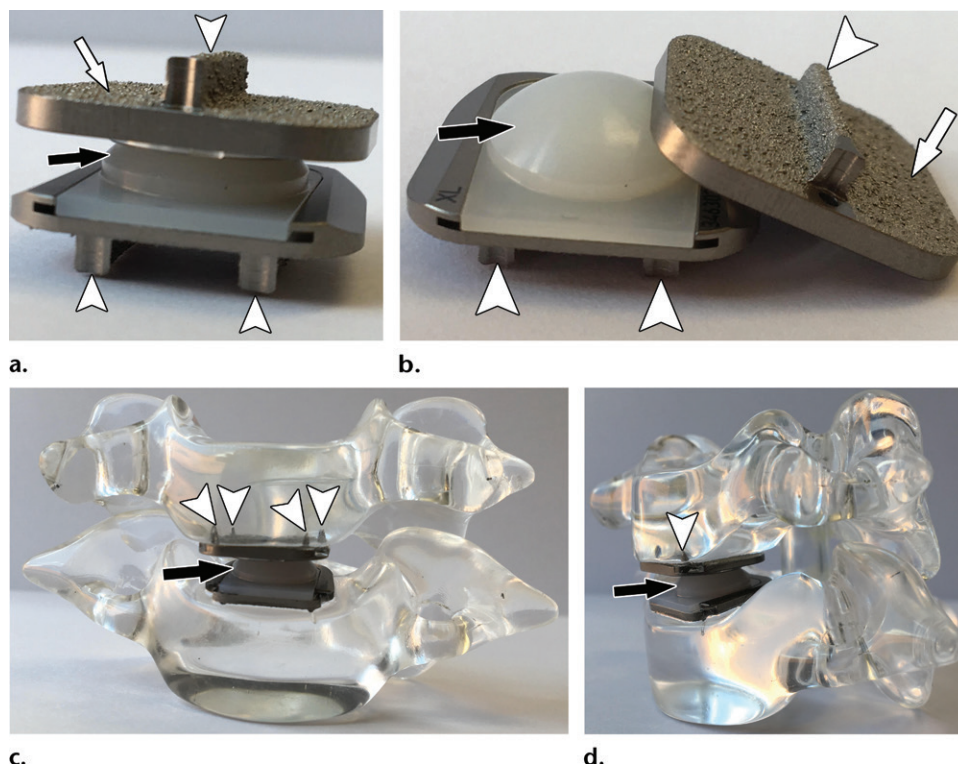


**Figure 11.** Two cervical disk prosthesis designs. (a, b) Photographs show an unconstrained design consisting of a ball-and-socket articulation (black arrow) and a bone-to-prosthesis interface featuring keels (arrowheads) and flat high-porosity surfaces (white arrow). (c, d) Photographs show an unconstrained design consisting of a ball-and-socket articulation (arrow) and a bone-to-prosthesis interface featuring spikes (arrowheads) and curved high-porosity surfaces. The curved high-porosity surfaces are hidden by the semitransparent spine model.

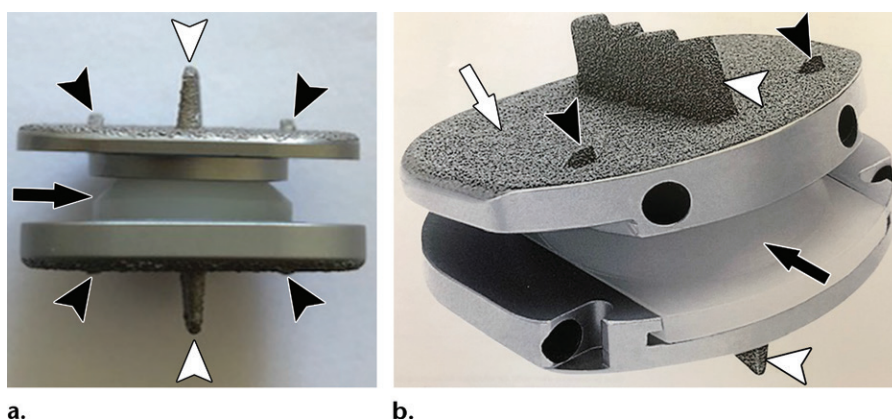


**Figure 12.** Lumbar disk prosthesis. Photographs show an unconstrained lumbar disk prosthesis design that consists of a ball-and-socket articulation (black arrow) and a bone-to-prosthesis interface featuring keels (white arrowheads), spikes (black arrowheads), and flat high-porosity surfaces (white arrow in b).

bodies in the setting of corpectomy for severe traumatic or tumor surgery (Fig 4) (39).

### Intervertebral Disk Replacements

Motion-preserving total intervertebral disk prostheses are an alternative to immobilizing osseous fusion-promoting intervertebral and spinal instrumentations (Figs 5, 6). Intervertebral disk replacement has the advantage that spinal seg-

mental motion is maintained after the procedure, whereas osseous fusion results in loss of segmental motion and increasing transmission of force to the adjacent segments.

Disk replacement prostheses typically consist of articulating polyethylene-bearing surfaces and two metallic endplate components, with keels and porous surfaces used to anchor into the superior and inferior host vertebral bodies (40) (Figs 5, 6).

Intervertebral disk prosthesis systems vary moderately in design, materials, bone-to-prosthesis interfaces, and articulation type (Figs 11, 12). A constrained-design intervertebral disk prosthesis consists of a bearing that contains a stopping mechanism within the normal physiologic range of motion, whereas an unconstrained-design prosthesis does not contain motion-restricting mechanisms. Most prostheses are made of alloys that contain cobalt and titanium, and polyethylene components.

A variety of bone-to-prosthesis interface structures are available to promote osseous integration into the host bone. These structures include keels, spikes, wire mesh, high-porosity surfaces, fixation screws, and surface coatings made of plasma-sprayed titanium, aluminum oxide, hydroxyapatite, and calcium phosphate. Articulation types can be differentiated into ball-and-socket articulation, which allows rotation around one individual point, and saddle articulation, which allows more than one center of rotation. Intervertebral disk replacements have been performed primarily in the cervical and lumbar spine and have not had widespread use (41,42).

### Indications for Postoperative CT

Indications for CT following spinal surgery include assessment of the type, integrity, and position of spinal implants. Other indications include delineation of the relationship of the implant(s) to the underlying spinal anatomy and abnormalities. Postoperative CT can also be used to assess the spinal alignment and effects of decompression surgery on the spinal canal and neural foramina, determine the success of intervertebral arthrodesis, and detect and characterize postoperative abnormalities (29).

### Normal Postoperative CT Findings

In the immediate postoperative period after spinal surgery, expected CT findings include soft-tissue edema and small amounts of gas and fluid along the surgical access site and around implants and instrumentation-treated spine segments. Seromas, another normal postoperative finding, are commonly observed simple collections in the surgical bed. When these collections are superficially located, they often are self-limiting and resorb over time (43).

Recombinant human BMP-2 at bone graft and interbody graft sites often incites an initial acute inflammatory response, which may result in focal osteolysis, limited endplate resorption at the graft site, and surrounding soft-tissue swelling (43,44).

Transpedicular screws should traverse the central portion of the pedicle and enter the vertebral body parallel to the endplate without breaching

the vertebral body cortex or having contact with neural elements and vascular structures. As an exception, sacral fixation screws may penetrate the anterior cortex for a short distance (15).

In cervical spinal instrumentation constructs, transpedicular C2 and C7 screws should have a horizontal orientation, extending anteriorly and slightly medially without breaching the pedicle cortex (4). Lateral mass screws in the C3–C7 vertebral bodies should have a superior and slightly lateral orientation (31). After ACDF, the anterior cervical plate should have a lordotic contour and be flush against the vertebral bodies. There should be a distance of at least 5 mm between the superior and inferior margins of the plate and the adjacent endplates to prevent periplate ossification (45). The screws should be fastened such that their heads are level with the plate.

In the setting of posterior spinal instrumentation constructs with screws and rods, the junction of the screw and rod should be carefully evaluated to ensure that the connector cap is completely fastened to the connector socket and the rod is engaged and aligned correctly. Angular malalignment of the rod in the connector can be a sign of construct instability (Fig 8).

An interbody graft is accurately positioned when the distance between the radiopaque marker of the posterior graft margin and the posterior vertebral body margin is 2 mm or greater (9,10,15) (Fig 13). When the interbody graft is placed closer than 2 mm to the posterior margin of the endplate, there is an increased risk of posterior migration into the spinal canal, with mass effect on the ventral thecal sac. Interbody grafts, especially stand-alone cages, may subside into the adjacent vertebral body for 3 mm or less before osseous fusion occurs (10).

Depending on the length of time since surgery, various degrees of osseous bridging across bone graft placement sites occur. At 6 months following discectomy with interbody graft placement, trabecular osseous bridging should be visible on CT images, either around or through the interbody graft (43) (Fig 3). Similarly, after posterolateral bone graft placement with pedicle screw and rod fixation, bridging bone should be visible between the transverse processes and facet joints (15,29). One year after surgery, mature trabeculation and solid cortical bridging should be present across the disk spaces (Fig 14) and posterolateral bone graft placement sites (Fig 4) (29,46).

On follow-up CT scans, asymptomatic granulation or scar tissue along the surgical tract and peridural spaces is part of the normal healing process (30,46). Epidural fibrosis typically has attenuation values that range from 50 to 75 HU and may partially resolve over time (46). Paraspinal muscle



**Figure 13.** Posterior interbody graft migration in a 69-year-old man who underwent posterior lumbar spinal instrumentation extending from the L3 to L5 vertebral bodies and including L3-L4 discectomy and interbody graft placement, posterior midline decompression, and pedicle screw and rod fixation (not shown). **(a)** Sagittal CT image obtained immediately following surgery shows successful placement of the L3-L4 interbody graft between the endplates, with a 2-mm distance between the posterior graft margin and posterior vertebral body margin (arrow). **(b)** Sagittal CT image obtained 6 weeks after surgery shows posterior migration of the interbody graft (arrow) into the central spinal canal, with mass effect on the ventral thecal sac.

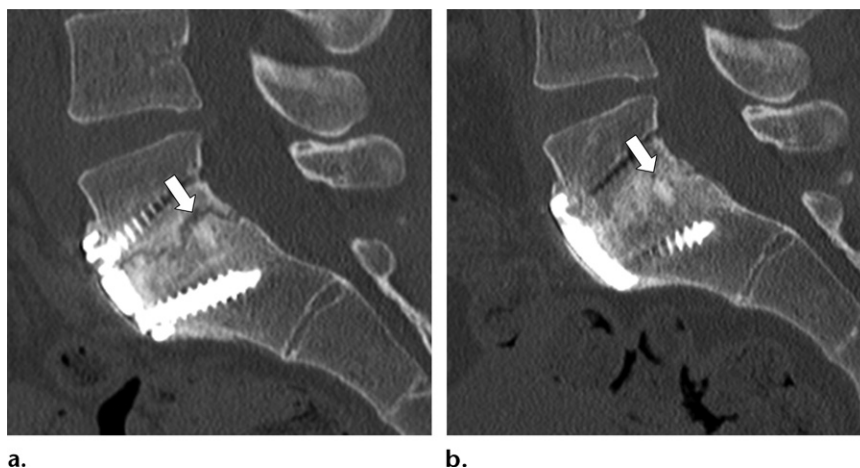
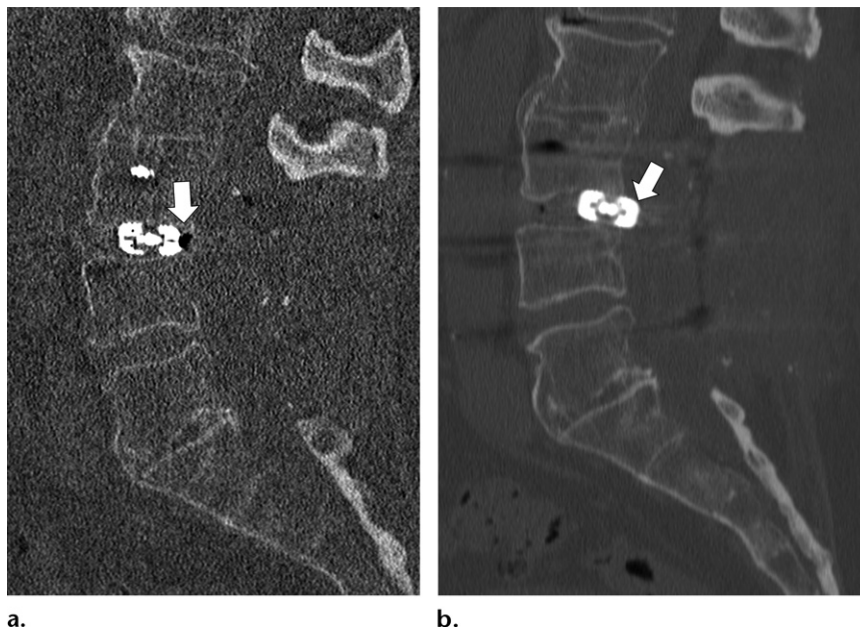


**Figure 14.** CT findings in a 29-year-old man with a history of L5-S1 spondylolysis and Meyerding grade I spondylolisthesis, who underwent lumbar spinal instrumentation of the L5-S1 motion segments, including discectomy with interbody graft placement and anterior plate and screw fixation. **(a)** Sagittal CT image obtained 39 weeks after surgery shows an irregular area of lucency (arrow) along the superior endplate-graft junction space, representing incomplete osseous integration and incomplete arthrodesis. **(b)** Sagittal CT image obtained 2 years after surgery shows complete osseous integration (arrow) along the endplate-graft interface and successful arthrodesis.

atrophy with fat replacement is a common finding following posterior surgical procedures (43).

## CT Appearances of Postoperative Spinal Complications

### Implant Placement

The position of the implant is important information gleaned from postoperative spinal CT. Any deviation from the expected position should be described (Fig 15). However, the clinical importance of variant implant positioning is usually unknown. Screws may breach the osseous cortex

and even come in contact with the thecal sac, neural elements, or paraspinal structures, causing symptoms or adverse clinical outcomes. Although pedicle screw breaches have been reported in up to 5.1% of cases, neurologic symptoms occur with a frequency of less than 0.2% (42). The most common cases of variant implant positioning are those involving misplaced pedicle screws.

Therefore, in the absence of visible injury to an adjacent structure or organ, we recommend using neutral descriptors to characterize implant positioning. This includes avoiding the use of words that denote blame or assign fault, such as *bad*,



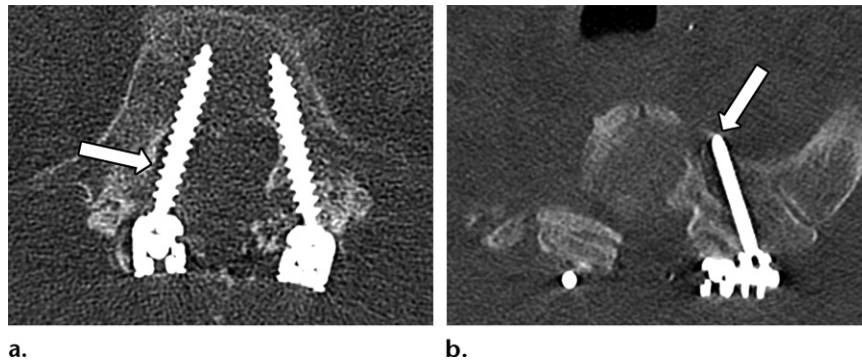


**Figure 15.** Variant screw placement. (a) Axial CT image at the L5 vertebral body level in a 71-year-old man who underwent lumbar spinal instrumentation of the L3–S1 motion segments, including midline decompression and posterior instrumentation with pedicle screws and vertical rods, shows a right pedicle screw (arrow) traversing the right lateral recess of the spinal canal. (b) Axial CT image at the T1 vertebral body level in a 60-year-old woman who underwent thoracic spinal instrumentation of the T1–T6 motion segments, including midline decompression and posterior instrumentation with pedicle screws and vertical rods, shows a left pedicle screw traversing the left articular process (arrow) lateral to the left pedicle.

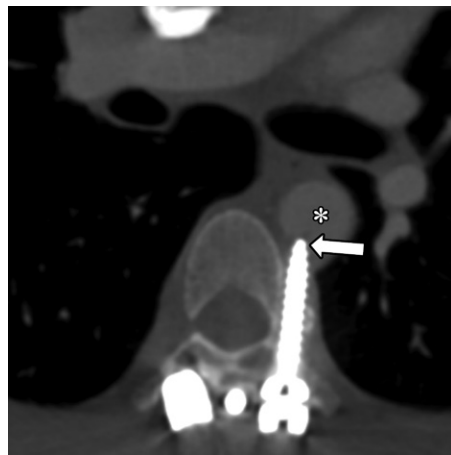


**Figure 16.** Variant placement of a thoracic pedicle screw in a 52-year-old man who underwent posterior spinal instrumentation extending from the occiput to the T8 vertebral body after resection of a cervical mass. Axial CT image shows the left T7 pedicle screw tip (arrow) reaching beyond the anterolateral vertebral body cortex to indent into the descending thoracic aorta (\*). Subsequently, a covered endovascular mesh stent graft was placed to minimize the risk of aortic injury.

*malpositioned*, and *misdirected*. For example, a description of a variant implant position could read as follows: “The left L1 pedicle screw tip abuts the posterior margin of the inferior vena cava, with preservation of adjacent fat planes.” This example accurately describes the hardware position, effect of the screw tip on the vena cava, and relevant additional findings such as preservation of adjacent fat planes, which implies that there is no radiologic evidence of injury. On this same token, findings of direct (eg, organ or vessel laceration) or indirect (fat stranding) injury to adjacent structures must be described and relayed in an emergent radiologist-to-surgeon communication.

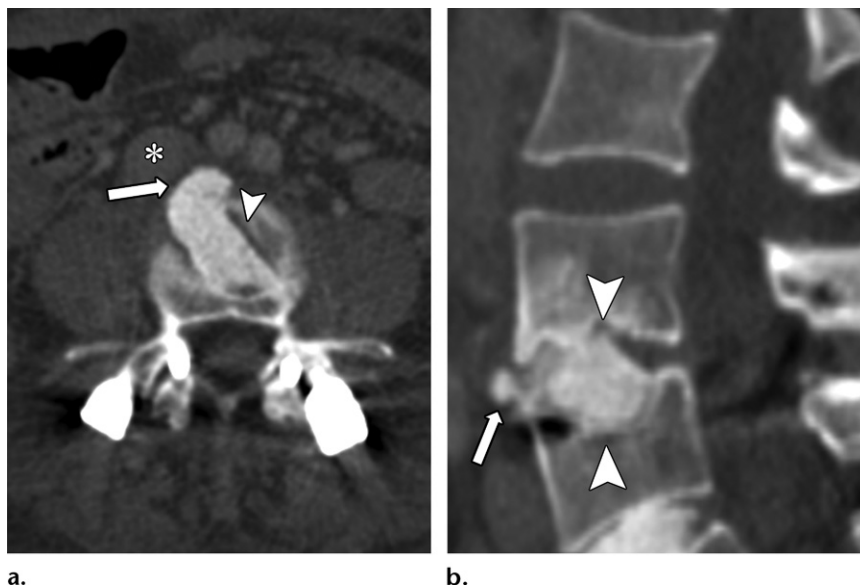
Medial angulation of pedicle screws, with breach of the medial cortex, may result in nerve root contact and irritation, the most common pedicle screw–related complication (6,15). In posterior cervical spine instrumentation, lateral angulation of the screw may breach the foramen transversarium and damage the vertebral artery (15). In posterior instrumentation of the thoracic and lumbar spine, the screw can traverse the anterior cortex and come in contact with retroperitoneal structures, leading to an immediate or delayed injury (Fig 16). Similarly, interbody cement grafts may extend beyond the vertebral body margin to adjacent structures (Fig 17).

The position of the interbody grafts and vertebral body plates may predict the development of future complications. Interbody grafts that are placed too close to the endplate margin may result in subsequent migration (15) (Figs 13, 18). A lateralized position of an interbody graft results in abnormal axial loading and abnormal spinal alignment (15). Placing an anterior plate within 5 mm of the adjacent endplate predisposes the patient to osteophyte formation (45).

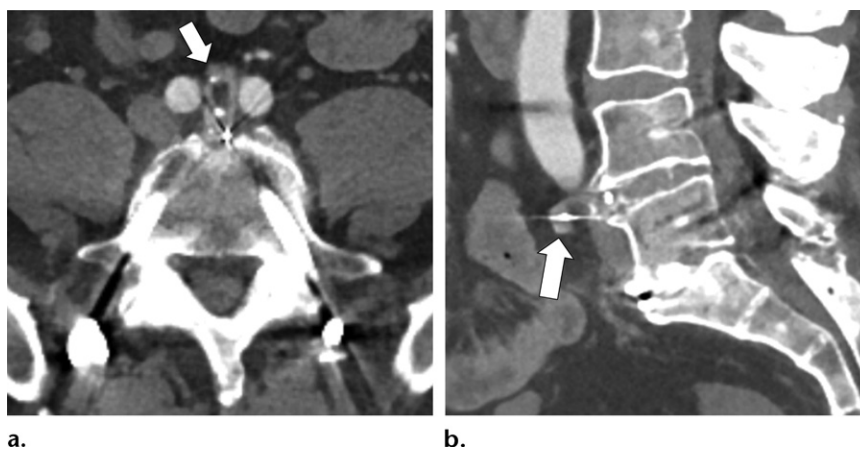
### Peri-implant Osteolysis

Evaluation for possible spinal implant loosening is performed according to principles that are similar to those for evaluating structures in other parts of the skeleton, such as the hip and knee following arthroplasty (47,48). Peri-implant osteolysis of the spine may be secondary to micromotion, infection, or a foreign body reaction to polyethylene and metal products (4,49) (Figs 19–21). In addition, the breakdown products of the BMP-2 that is used in conjunction with interbody grafts can cause temporary endplate osteolysis (50). Circumferential peri-implant osteolysis around spinal

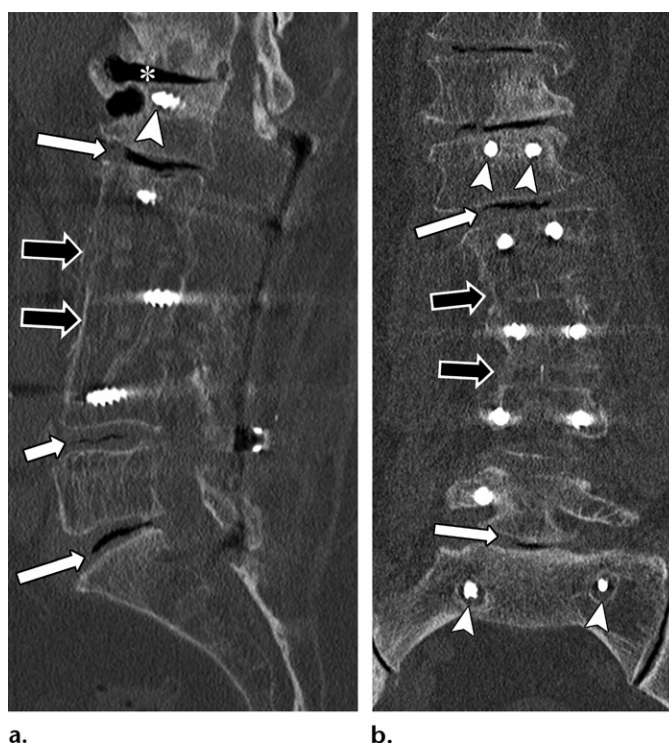
**Figure 17.** Periprosthetic osteolysis and graft migration in a 47-year-old man who underwent posterior lumbar spinal instrumentation extending from the L4 to S1 vertebral bodies, with interbody cement graft placement, posterior midline decompression, and pedicle screw and rod fixation. Axial (a) and sagittal (b) CT images show anterior extension of the interbody cement graft (arrow), which is in contact with the right common iliac vein (\* in a), as well as osteolysis along the graft-endplate interfaces (arrowheads), with subsidence.

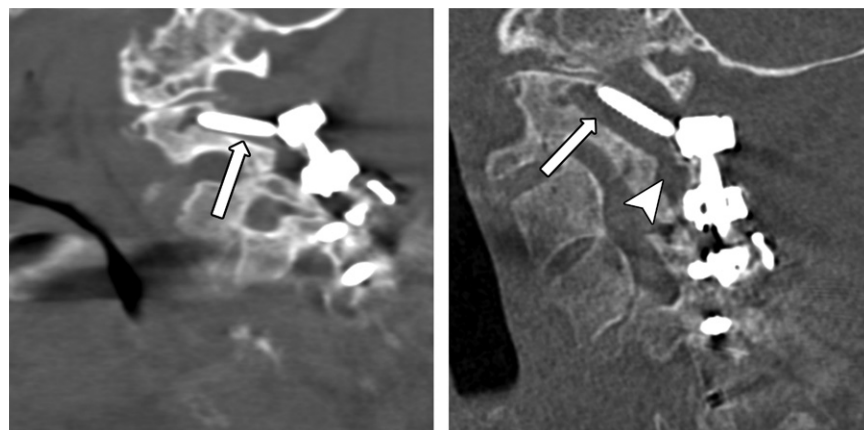


**Figure 18.** Interbody graft migration in a 52-year-old man who underwent posterior lumbar spinal instrumentation from the L4 to S1 vertebral bodies, including discectomy and interbody graft placement. Axial (a) and sagittal (b) CT images show anterior displacement of the L4-L5 interbody graft (arrow), which lies immediately inferior to the aortic bifurcation and comes in contact with the proximal right and left common iliac arteries.



**Figure 19.** CT findings in a 70-year-old man who continued to have back pain after lumbar spinal instrumentation extending from the L1 to S1 motion segments, including posterior midline decompression, L2-L3 and L3-L4 discectomies with interbody graft placements, and pedicle screw and rod fixation 8 years earlier. Sagittal (a) and coronal (b) CT images show osteolysis around the L1 and S1 pedicle screws (arrowheads) and L1-L2, L4-L5, and L5-S1 vacuum cleft phenomena (white arrows), suggesting micromotion as an explanation for unsuccessful arthrodesis. The L2-L3 and L3-L4 arthrodeses (black arrows) were successful, as indicated by the solid osseous bridging across the disk spaces. Adjacent segment disease with severe disk degeneration (\* in a) also is seen.





a.

b.

**Figure 20.** Periprosthetic osteolysis and implant migration in a 66-year-old man who underwent posterior spinal instrumentation extending from the C2 to T2 vertebral bodies, with midline decompression and rod and pedicle screw fixation. (a) Sagittal CT image shows osteolysis (arrow) around the right C2 screw, which suggests impaired osseous fixation. (b) Sagittal CT image obtained at 16-month follow-up shows progressive osteolysis (arrow) and angular migration of the right C2 screw, with extension into the right C1-C2 facet joint (arrowhead).



**Figure 21.** Variant screw placement in a 71-year-old man who underwent posterior cervicothoracic spinal instrumentation starting at the C3 vertebral body. Sagittal CT image shows a lack of osseous purchase (arrow) of the right C3 lateral mass screw, with the tip reaching the right C2-C3 facet joint, and retraction of the instrumentation construct (arrowhead).

implants larger than 2 mm suggests implant loosening (51). However, to diagnose implant loosening with certainty, a change in the position of the implant must be demonstrated at serial imaging. Sclerosis around a screw is highly suggestive of an adaptive response to prior hardware loosening. Implant migration may result in a change in spinal alignment, such as increasing anterolisthesis in the setting of a loose pedicle screw (Fig 22).

Because infection can manifest with peri-implant osteolysis, it is important to distinguish infection from mechanical loosening; however, this can be challenging. The pattern of peri-implant osteolysis can help differentiate an infectious cause

from a mechanical loosening-related cause. With mechanical loosening of a screw, the osteolysis may be more prominent along the distal tip owing to a pivot point around which the screw moves, whereas infectious osteolysis is often more diffuse (Fig 23). However, because the CT appearances of mechanical loosening-related osteolyses and those of infection-related osteolyses overlap, correlation of the CT appearance with the clinical presentation, laboratory values, prior imaging study findings, and/or radionuclide imaging findings is often part of the workup (29,45). The inflammatory effects of using recombinant human BMP-2 can result in inflammatory stranding of soft tissues and abnormal enhancement and thus mimic infection on CT images of the postoperative spine (29).

Loosening and motion of spinal implants are important contributors to unsuccessful intervertebral arthrodesis, pseudoarthrosis, and non-union, which are visible on CT images owing to the lack of mature osseous bridging 1 year after surgery. Pseudoarthrosis may cause pain and increased implant stress that ultimately leads to implant failure (52). Radiographically, a greater than 2-mm change in the interspinous distance and a 2° or greater change in Cobb angle measurements are functionally diagnostic of pseudoarthrosis (52). At CT, pseudoarthrosis manifests as a lucent line through the intervertebral bone graft material or along the graft postoperative interface, with or without adjacent sclerosis (Figs 14, 24, 25). Following interbody graft placement, subcortical cysts, vacuum cleft phenomena (Figs 14, 24), and lack of mature trabeculations across the disk space 24 months following surgery are additional signs that suggest micromotion and



**Figure 22.** Periprosthetic osteolysis and implant migration in a 33-year-old woman who underwent posterior cervical spinal instrumentation from the C3 to C7 vertebral bodies, including midline decompression and screw and rod fixation. (a) Sagittal CT image shows osteolysis (arrow) around the left lateral mass screw of the C3 vertebral body, with screw retraction (arrowhead) and suggested impaired osseous fixation. (b) Sagittal CT image obtained at 3-month follow-up shows progression of the osteolysis (arrow), increasing screw retraction, and slightly increasing C3-C4 anterolisthesis (arrowhead).

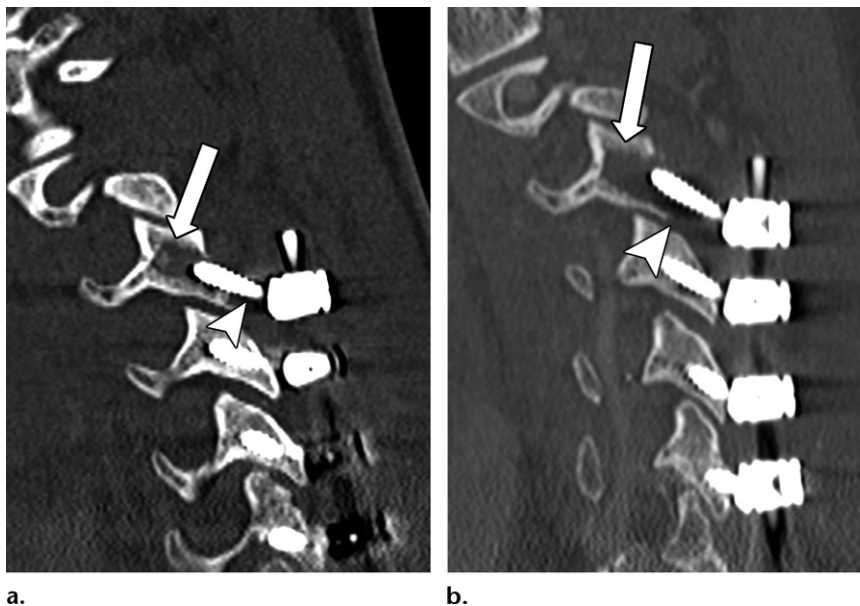


**Figure 23.** Periprosthetic osteolysis and implant displacement in a 31-year-old man who underwent anterior cervical spinal instrumentation, including C6-C7 discectomy with anterior plate and screw fixation, C5-T1 midline decompression, and posterior screw and rod fixation. (a) Axial CT image shows geographic osteolysis around the anterior right C6 vertebral screw (arrow) due to infection. (b) Oblique volume-rendered image shows displacement of the left C6 screw (arrowhead) into the prevertebral soft tissue.

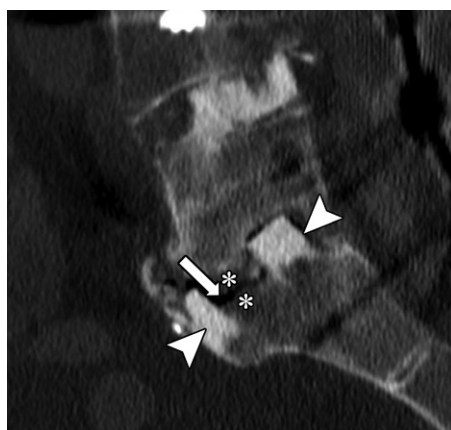
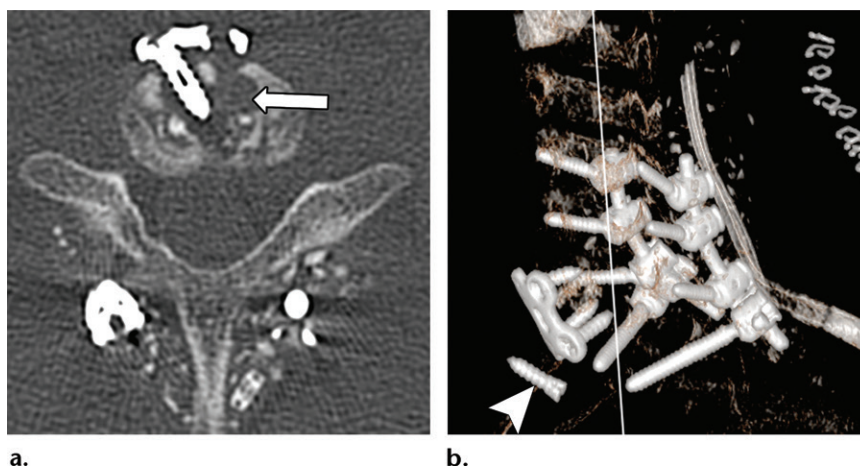


**Figure 24.** Intervertebral pseudoarthrosis. Sagittal CT image shows so-called “locked” pseudoarthrosis, which is characterized by attempted but incomplete osseous bridging through the interbody graft (arrowheads), where a nonossified layer remains between the opposing ossified columns (\*). The presence of a vacuum cleft phenomenon (arrow) at the nonossified layer and graft-endplate interface suggests motion and segmental microinstability.

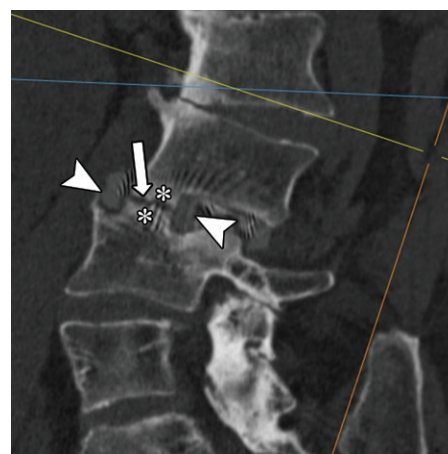


**Figure 25.** Intervertebral pseudoarthrosis. Sagittal CT image shows locked pseudoarthrosis, which is characterized by attempted but incomplete osseous bridging through the interbody graft (arrowheads), where a nonossified layer (arrow) remains between the opposing ossified columns (\*). The absence of a vacuum cleft phenomenon at the nonossified layer and graft-endplate interface suggests segmental stability.



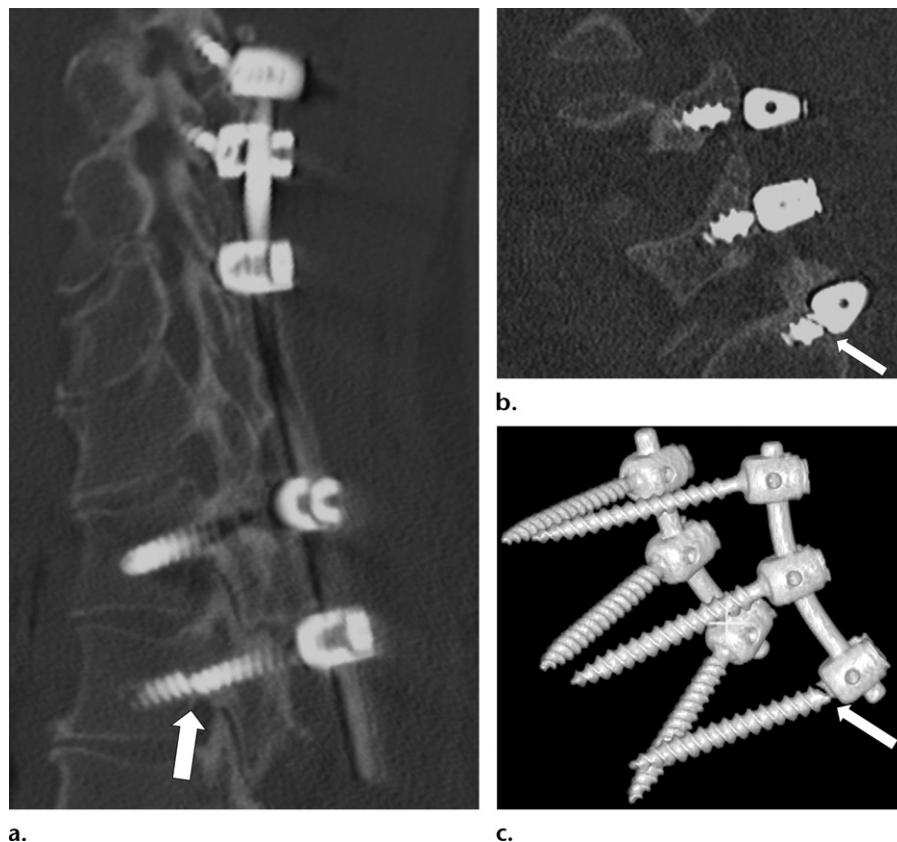


**Figure 26.** Screw fractures in two patients. (a) Sagittal CT image in a 66-year-old woman shows a fracture (arrow) of a left T2 screw shaft in the pedicle, with minimal displacement. (b, c) Sagittal (b) and oblique volume-rendered (c) CT images in a 78-year-old man show a neck fracture (arrow) of a left S1 screw. Screw fractures may be better depicted on volume-rendered CT images.

pseudoarthrosis. Interbody graft migration, subsidence, resorption, and fracture after interbody graft placement also may suggest micromotion and pseudoarthrosis (Figs 24, 25) (29,51). In addition, failed coalition of osseous fragments and absence of bridging bone at posterolateral bone graft placement sites and in posterior elements 24 months after spinal instrumentation suggest nonunion (29).

### Implant Failure

Implants can fail owing to a number of mechanisms. The implant itself can become fractured as a result of fatigue caused by repetitive stress (Fig 26) (10). Three-dimensional postprocessing can help to detect minimally displaced implant fractures. Fractured implants may result in micromotion and segmental microinstability, which interfere with the progression of osseous fusion (Fig 27). Although the implant may be intact, there can be mechanical disengagement of screws, bolts, and/or rods, such as those used in posterior fixations (Fig 8). In extreme cases, there can be loosening of a cap with a completely unsecured rod (Fig 28). In plate and screw fixation constructs, screws should engage with the plate to ensure compression. However, when there are multiple screws, a single failing screw may not interfere with the stability of the construct, and osseous fusion still may occur (Fig 29).

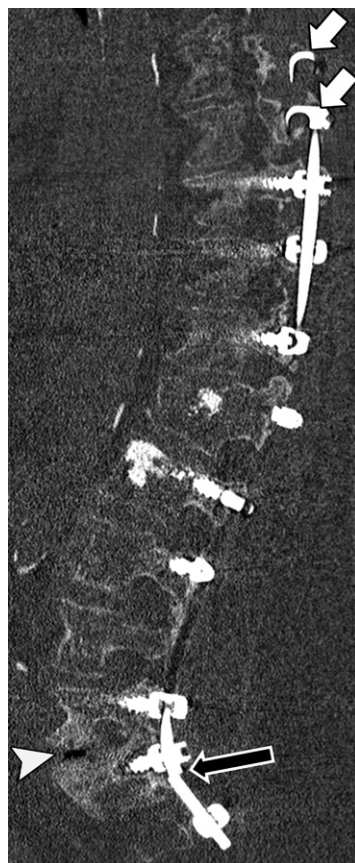


**Figure 27.** Rod fracture in a 69-year-old woman who underwent posterior lumbar spinal instrumentation extending from the T8 to S2 motion segments, with disengaged hooks at the T8-T9 level (white arrows), a fractured rod at the S1 level (black arrow), osteolysis around the S1 screw, and a vacuum cleft phenomenon (arrowhead) of the L5-S1 disk space, indicating micromotion and segmental instability.

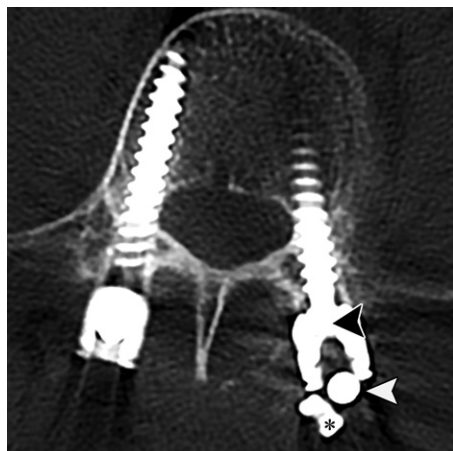


**Figure 28.** Rod disengagement in a 77-year-old woman who underwent posterior lumbar spinal instrumentation extending from the L3 to S1 vertebral bodies. Axial CT image shows rod disengagement of the left S1 pedicle screw (white arrowhead) due to displacement of the locking head screw (\*) from the connector socket (black arrowhead).

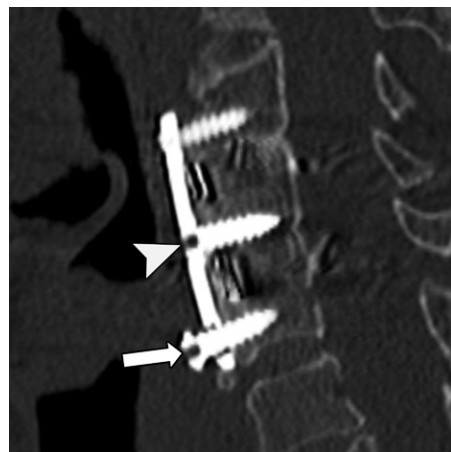


**Figure 29.** Sagittal CT image obtained after cervical discectomy with interbody graft placement and anterior plate and screw fixation of the C3–C5 motion segments shows an incompletely engaged screw (arrow) at the C5 level and a successfully engaged screw (arrowhead) superiorly. There is successful intervertebral arthrodesis, as indicated by the complete osseous bridging across the disk spaces.

Migration and subsidence of failing implants can cause spinal canal and neuroforaminal narrowing, pseudoarthrosis, instability, and adjacent segment degeneration. A small degree of subsidence of interbody grafts and cages into the adjacent endplate is expected. However, subsidence exceeding 3 mm in depth can narrow the disk space and neural foramen enough to cause radicular pain (Fig 30) (15,52). Given the current use of titanium and polyetheretherketone implants, streak artifacts no longer significantly limit the detection of subsidence (29).

### Fractures around Implants and Prostheses

Owing to weakened bone strength secondary to osteolysis, prior bone resection, and/or increased biomechanical loading through a fixation construct, osseous fractures can occur around any spinal implant or prosthesis that is embedded in bone (Figs 31, 32). Fracture descriptors that are helpful to the surgeon include orientation of the fracture line, degree of comminution, extension of the fracture line to articular surfaces and foramina, abnormal alignment, and additional abnormalities in the spine.

### Adjacent Segment Disease

Adjacent segment disease is the development or progression of motion segment degeneration directly above and below a spinal instrumentation construct (10). In adjacent segment disease, the degeneration is accelerated secondarily to the summation of forces and resultant increased transmission of the biomechanical load from the instrumentation-managed and immobilized spinal



**Figure 30.** CT findings in a 71-year-old man who presented with persistent low back pain after undergoing lumbar spinal instrumentation of the L4–L5 motion segment, including discectomy with interbody graft placement and posterior plate and screw fixation, approximately 6 months ago. Coronal CT image shows a vacuum cleft phenomenon (arrow) of the L4–L5 interspace, as well as greater than 3-mm abnormal graft migration into the endplate with surrounding osteolysis (arrowheads), indicating micromotion and a lack of osseous integration.



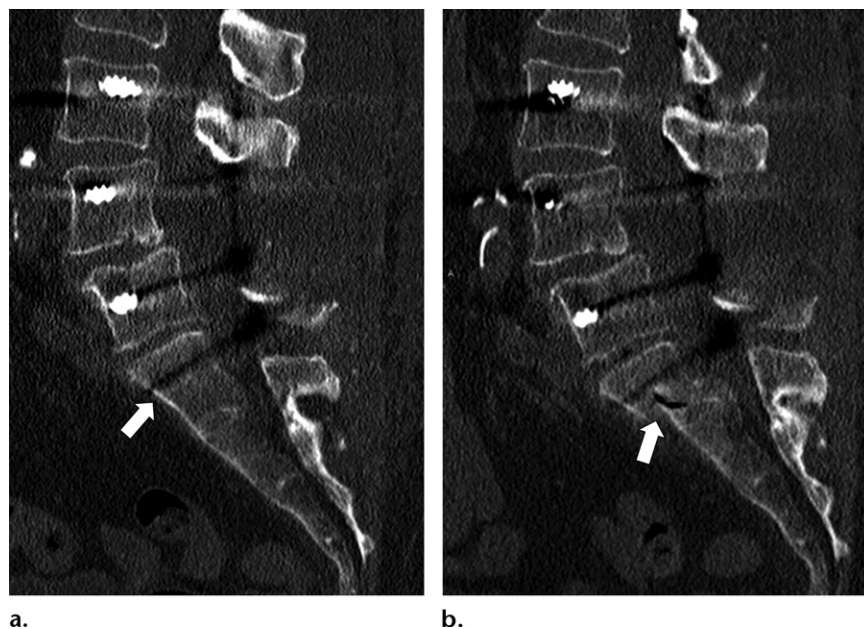


**Figure 31.** Periprosthetic bone fracture in a 77-year-old woman who underwent posterior lumbar spinal instrumentation extending from the L3 to S1 vertebral bodies. (a) Sagittal CT image obtained 1 day after the instrumentation surgery shows baseline alignment, with an intact S1 vertebral body (arrow). (b) Sagittal CT image obtained 1 month after the surgery shows a new fracture (arrow) of the adjacent S1 segment, with anterior displacement.

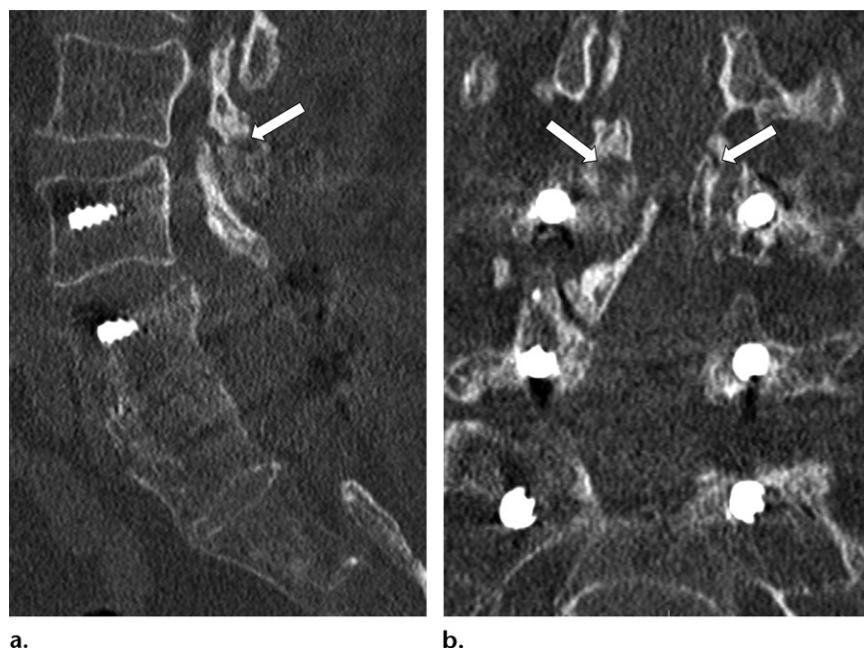


**Figure 32.** Periprosthetic fracture in a 73-year-old woman who underwent posterior lumbar spinal instrumentation from the L4 to S1 vertebral bodies, including midline decompression and pedicle screw and rod fixation. Sagittal (a) and coronal (b) CT images show fractures (arrows) of the right and left articular processes of the adjacent L3 vertebral body.

segments. These segments act as a lever arm and exert torque forces at the levels of the adjacent native motion segments above and below the instrumentation construct. CT findings include disk degeneration and facet joint arthrosis, which may progress to spinal stenosis. Adjacent segment disease is more common in the lumbar spine and at the levels above the instrumentation-managed segment (Fig 19) (10,15).

### Collections and Fistulas

After spinal surgery, postoperative collections are common and include seroma, hematoma, abscess, and pseudomeningocele, which may be

symptomatic or incidental findings (25). Accurate differentiation of the various collection types is important for implementing the most appropriate management.

A postoperative hematoma is a focal collection of blood products, which may be located within or around the spinal canal or implant, and/or along the surgical access. Hematomas commonly develop in the subcutaneous tissue, and typically no intervention is required in such cases. The majority of postoperative hematomas develop within hours to days after surgery. The symptoms that result from postoperative hemorrhage are based on the location of the collection.

**Figure 33.** Postoperative collections in a 68-year-old woman who underwent posterior spinal instrumentation from the T4 to S1 vertebral bodies, including midline decompression of the L2–L4 vertebral bodies. Sagittal (a) and axial (b) CT images of the lumbar spine at the L3–L4 level show a low-attenuation collection (arrows), representing a postsurgical seroma, in the posterior decompression bed.

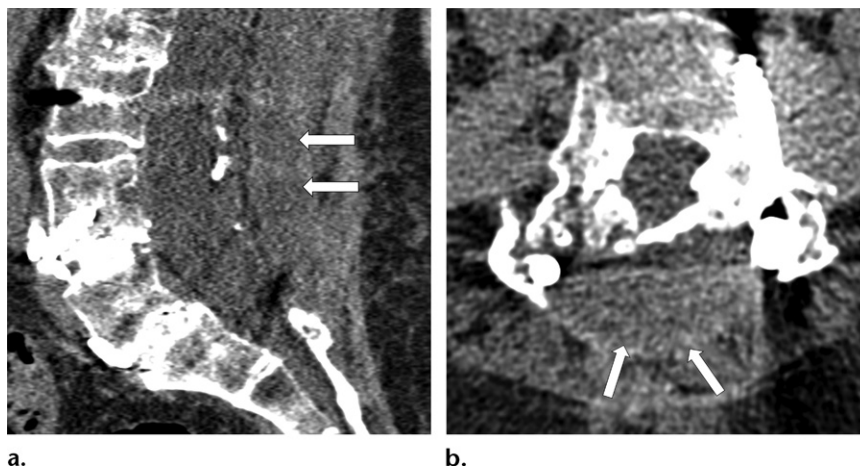
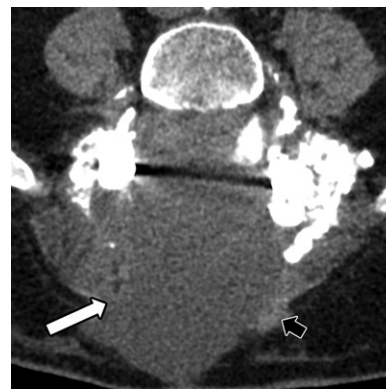


**Figure 34.** Postoperative collection in a 70-year-old man who underwent posterior lumbar spinal instrumentation extending from the L4 to S1 vertebral bodies, including midline decompression, interbody graft placements, and posterior pedicle screw and rod fixation. Axial CT image obtained at the L4–L5 level shows a large hypoattenuating collection (white arrow) in the area of the midline decompression and surgical access, without separation from the thecal sac. The border of the collection consists of reactive fibrous tissue (black arrow), which is suggestive of a pseudomeningocele. Head MRI (not shown) demonstrated signs of intracranial hypotension, and lumbar spine MRI (not shown) depicted a small dural defect with cerebrospinal fluid leakage at the L4–L5 level, confirming a pseudomeningocele.



Epidural and subdural spinal hematomas can exert mass effect on neural elements and may cause pain and neurologic deficits. However, the incidence of symptomatic epidural hematomas is commonly overestimated, with the actual incidence ranging between 0.1% and 1.0% (53). Non-contrast material-enhanced CT depicts a clotted hematoma as a high-attenuation extradural collection with a biconvex shape (54). The high-attenuation collection is distinct from the adjacent low-attenuation epidural fat and spinal cord (54). Epidural hematomas often occur dorsolateral to the spinal cord. Subdural hemorrhages are uncommon, with only a few cases reported.

A postoperative seroma (Fig 33) is a collection of clear serous fluid that contains blood plasma or inflammatory fluid from severed small blood vessels or soft tissues, respectively (55). The collection can be located in the subcutaneous or paraspinal tissues. The use of BMP has been associated with an increased risk of postoperative seroma (56). Treatments include the use of a compression bandage for smaller seromas and percutaneous or surgical drainage for large, symptomatic, and infected seromas (25). CT attenuation measurements may be used to differentiate seromas from hematomas. However, MRI is more accurate in areas without impeding metal artifacts (51).

### Pseudomeningoceles and Dural Leakage

A pseudomeningocele (Fig 34) is an abnormal collection of cerebrospinal fluid in paraspinal regions that communicate with the cerebrospinal fluid space around the spinal cord through a meningeal defect. Pseudomeningoceles occur in fewer than 2% of patients following laminectomy or discectomy (57). Pseudomeningoceles can be symptomatic owing to mass effect and accompanied by intracranial hypotension and meningitis related to cerebrospinal fluid hypovolemia. The border of a pseudomeningocele, unlike that of a true meningocele, consists of reactive fibrous tissue (Fig 34) (25). Pseudomeningoceles can extend from the spinal canal through a posterior defect at the site of resected posterior elements. On CT images, a pseudomeningocele typically appears as a hypoattenuating collection that extends to the dura, with minimal peripheral enhancement. At laminotomy and laminectomy sites, the dural sac may protrude posteriorly and should not be mistaken for a pseudomeningocele (15). CT myelography can be helpful for differentiating a communicating pseudomeningocele from a seroma and visualizing dural leaks (58). The CT-guided injection of iodine-based contrast material into the subarachnoid space can be helpful for visualizing a defect, as indicated by



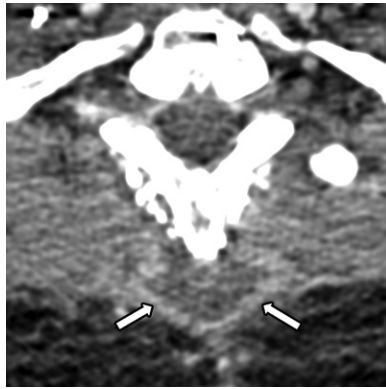
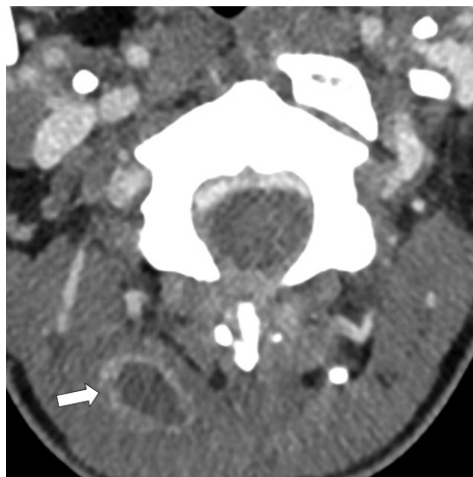
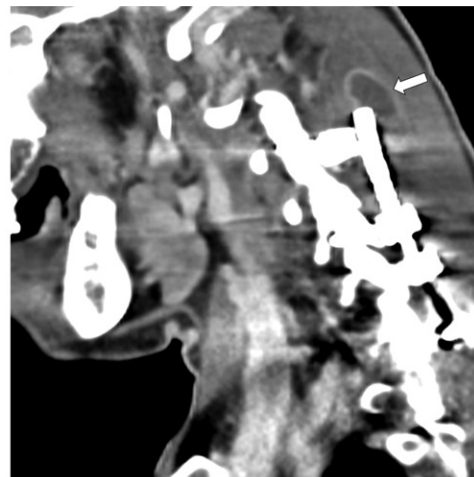


**Figure 35.** Paraspinal abscesses in a 31-year-old man who underwent posterior cervicothoracic instrumentation extending from the C5 to T1 vertebral bodies. Axial CT image obtained after the intravenous administration of iodine-based contrast material shows a rim-enhancing collection (arrows), representing a soft-tissue abscess, posterior to the spinous processes, with adjacent fat stranding.



a.



b.

**Figure 36.** CT findings in a 33-year-old man who underwent posterior cervical instrumentation extending from the C4 to C7 vertebral bodies. Axial (a) and coronal (b) CT images obtained after the intravenous administration of iodine-based contrast material, with iterative metal artifact reduction postprocessing, show a rim-enhancing collection (arrow) cranial to the right rod, representing a soft-tissue abscess.

iodine-based contrast material traversing into a pseudomeningocele.

### Surgical Site Infection and Abscess

Surgical site infection is an important complication that occurs most commonly during the 1st month following spinal surgery. Causes of these infections include direct contamination during surgery, hematogenous seeding, and implant-associated infection (59). Patient-related risk factors include diabetes mellitus, smoking, renal failure, malnutrition, immunosuppression, obesity, and older age (60). Surgery-related risk factors include lengthy surgery, prolonged retraction, implant placement, and bone graft placement (59). The most common infecting organisms are *Staphylococcus aureus* and gram-negative bacteria (59).

Although MRI is more accurate than CT for evaluation of postoperative fluid collections, contrast-enhanced CT can be used to detect rim-enhancing abscesses within the surgical bed and paraspinal musculature (Figs 35, 36). Additional findings include paraspinal edema and phlegmon,

muscular enhancement, vertebral body destruction, and gas formation in the soft tissue and bone (25).

### Conclusion

CT is an important modality for evaluating the success of spinal instrumentation surgery and detecting postoperative complications. The use of optimized CT protocols and advanced metal artifact reduction techniques can facilitate substantially reduced artifacts and improved image quality. CT is accurate for determining the location and integrity of implants and identifying peri-implant osteolysis, fractures, and adjacent segment disease. CT can depict collections and often can be used to diagnose abscesses. However, myelography and MRI are often needed to fully characterize and diagnose fistulas, pseudomeningoceles, and surgical site infections. Familiarity with spinal implants, spinal surgical techniques, normal postoperative spine appearances, and various related complications will aid in accurately interpreting postoperative CT findings and guiding medical, surgical, and interventional management.

**Acknowledgment.**—The authors thank Hannah Ahn for creating the drawings in Figures 2 and 7.

**Disclosures of Conflicts of Interest.**—**E.K.F.** *Activities related to the present article:* disclosed no relevant relationships. *Activities not related to the present article:* research support from Siemens and GE Healthcare, co-founder and stockholder in HipGraphics. *Other activities:* disclosed no relevant relationships. **M.F.** *Activities related to the present article:* disclosed no relevant relationships. *Activities not related to the present article:* board member of and shareholder in Incemed and Prognosyst. *Other activities:* disclosed no relevant relationships. **J.F.** *Activities related to the present article:* disclosed no relevant relationships. *Activities not related to the present article:* grants or grants pending, payment for lectures (including service on speakers bureaus), and payment for travel and meeting expenses from Siemens; grants or grants pending from BTG International. *Other activities:* patent(s) or copyright(s) pending, and patent(s) or copyright(s) issued from Siemens.

## References

- Martin BI, Mirza SK, Spina N, Spiker WR, Lawrence B, Brodtkie DS. Trends in Lumbar Fusion Procedure Rates and Associated Hospital Costs for Degenerative Spinal Diseases in the United States, 2004 to 2015. *Spine* 2019;44(5):369–376.
- Liu CY, Zygorakis CC, Yoon S, et al. Trends in Utilization and Cost of Cervical Spine Surgery Using the National Inpatient Sample Database, 2001 to 2013. *Spine* 2017;42(15):E906–E913.
- Hoy D, Bain C, Williams G, et al. A systematic review of the global prevalence of low back pain. *Arthritis Rheum* 2012;64(6):2028–2037.
- Petscavage-Thomas JM, Ha AS. Imaging current spine hardware. I. Cervical spine and fracture fixation. *AJR Am J Roentgenol* 2014;203(2):394–405.
- Krumme JW, Lauer MF, Stowell JT, Beteslasi NM, Kotwal SY. Bone Scintigraphy: A Review of Technical Aspects and Applications in Orthopedic Surgery. *Orthopedics* 2019;42(1):e14–e24.
- Berquist TH. Imaging of the postoperative spine. *Radiol Clin North Am* 2006;44(3):407–418.
- McLellan AM, Daniel S, Corcuera-Solano I, Joshi V, Tanenbaum LN. Optimized imaging of the postoperative spine. *Neuroimaging Clin N Am* 2014;24(2):349–364.
- Katsura M, Sato J, Akahane M, Kunimatsu A, Abe O. Current and Novel Techniques for Metal Artifact Reduction at CT: Practical Guide for Radiologists. *RadioGraphics* 2018;38(2):450–461.
- Rutherford EE, Tarplett LJ, Davies EM, Harley JM, King LJ. Lumbar spine fusion and stabilization: hardware, techniques, and imaging appearances. *RadioGraphics* 2007;27(6):1737–1749.
- Thakkar RS, Malloy JP 4th, Thakkar SC, Carrino JA, Khanna AJ. Imaging the postoperative spine. *Radiol Clin North Am* 2012;50(4):731–747.
- Splendiani A, D'Orazio F, Patriarca L, et al. Imaging of post-operative spine in intervertebral disc pathology. *Musculoskelet Surg* 2017;101(Suppl 1):75–84.
- Fritz J, Fishman EK, Small KM, et al. MDCT arthrography of the shoulder with datasets of isotropic resolution: indications, technique, and applications. *AJR Am J Roentgenol* 2012;198(3):635–646.
- Calhoun PS, Kuszyk BS, Heath DG, Carley JC, Fishman EK. Three-dimensional volume rendering of spiral CT data: theory and method. *RadioGraphics* 1999;19(3):745–764.
- Khodarahmi I, Fishman EK, Fritz J. Dedicated CT and MRI Techniques for the Evaluation of the Postoperative Knee. *Semin Musculoskelet Radiol* 2018;22(4):444–456.
- Bittane RM, de Moura AB, Lien RJ. The postoperative spine: what the spine surgeon needs to know. *Neuroimaging Clin N Am* 2014;24(2):295–303.
- Khodarahmi I, Haroun RR, Lee M, et al. Metal Artifact Reduction Computed Tomography of Arthroplasty Implants: Effects of Combined Modeled Iterative Reconstruction and Dual-Energy Virtual Monoenergetic Extrapolation at Higher Photon Energies. *Invest Radiol* 2018;53(12):728–735.
- Dangelmaier J, Schwaiger BJ, Gersing AS, et al. Dual layer computed tomography: Reduction of metal artefacts from posterior spinal fusion using virtual monoenergetic imaging. *Eur J Radiol* 2018;105:195–203.
- Guggenberger R, Winklhofer S, Osterhoff G, et al. Metallic artefact reduction with monoenergetic dual-energy CT: systematic ex vivo evaluation of posterior spinal fusion implants from various vendors and different spine levels. *Eur Radiol* 2012;22(11):2357–2364.
- Kotsenas AL, Michalak GJ, DeLone DR, et al. CT Metal Artifact Reduction in the Spine: Can an Iterative Reconstruction Technique Improve Visualization? *AJNR Am J Neuroradiol* 2015;36(11):2184–2190.
- Rowe SP, Fritz J, Fishman EK. CT evaluation of musculoskeletal trauma: initial experience with cinematic rendering. *Emerg Radiol* 2018;25(1):93–101.
- Slone RM, MacMillan M, Montgomery WJ. Spinal fixation. I. Principles, basic hardware, and fixation techniques for the cervical spine. *RadioGraphics* 1993;13(2):341–356.
- Slone RM, MacMillan M, Montgomery WJ, Heare M. Spinal fixation. II. Fixation techniques and hardware for the thoracic and lumbosacral spine. *RadioGraphics* 1993;13(3):521–543.
- Mobbs RJ, Phan K, Malham G, Seex K, Rao PJ. Lumbar interbody fusion: techniques, indications and comparison of interbody fusion options including PLIF, TLIF, MI-TLIF, OLIF/ATP, LLIF and ALIF. *J Spine Surg* 2015;1(1):2–18.
- Kani KK, Chew FS. Anterior cervical discectomy and fusion: review and update for radiologists. *Skeletal Radiol* 2018;47(1):7–17.
- Bellini M, Ferrara M, Grazzini I, Cerase A. Neuroimaging of the Postoperative Spine. *Magn Reson Imaging Clin N Am* 2016;24(3):601–620.
- Moser M, Farshad M, Farshad-Amacker NA, Betz M, Spirig JM. Accuracy of Patient-Specific Template-Guided Versus Freehand Cervical Pedicle Screw Placement from C2 to C7: A Randomized Cadaveric Study. *World Neurosurg* 2019;S1878–S8750(19)30575–3. doi: 10.1016/j.wneu.2019.02.152. Accessed August 18, 2019.
- Geer CP, Papadopoulos SM. The argument for single-level anterior cervical discectomy and fusion with anterior plate fixation. *Clin Neurosurg* 1999;45:25–29; discussion 21.
- Young PM, Berquist TH, Bancroft LW, Peterson JJ. Complications of spinal instrumentation. *RadioGraphics* 2007;27(3):775–789.
- Zampolin R, Erdfarb A, Miller T. Imaging of lumbar spine fusion. *Neuroimaging Clin N Am* 2014;24(2):269–286.
- Ha AS, Petscavage-Thomas JM. Imaging of current spinal hardware: lumbar spine. *AJR Am J Roentgenol* 2014;203(3):573–581.
- Murtagh RD, Quencer RM, Castellvi AE, Yue JJ. New techniques in lumbar spinal instrumentation: what the radiologist needs to know. *Radiology* 2011;260(2):317–330.
- Quinn JC, Patel NV, Tyagi R. Hybrid lateral mass screw sublaminar wire construct: A salvage technique for posterior cervical fixation in pediatric spine surgery. *J Clin Neurosci* 2016;25:118–121.
- Pizones J, Sánchez-Mariscal F, Zúñiga L, Izquierdo E. The effect of sublaminar wires on the rib hump deformity during scoliosis correction manoeuvres. *Eur J Orthop Surg Traumatol* 2016;26(7):771–777.
- Harrington PR. Treatment of scoliosis: correction and internal fixation by spine instrumentation. *J Bone Joint Surg Am* 1962;44-A(4):591–610.
- Luque ER. Segmental spinal instrumentation for correction of scoliosis. *Clin Orthop Relat Res* 1982;(163):192–198.
- Yazici M, Olgun ZD. Growing rod concepts: state of the art. *Eur Spine J* 2013;22(suppl 2):S118–S130.
- Akbarnia BA, Pawelek JB, Cheung KM, et al. Traditional Growing Rods Versus Magnetically Controlled Growing Rods for the Surgical Treatment of Early-Onset Scoliosis: A Case-Matched 2-Year Study. *Spine Deform* 2014;2(6):493–497.
- Kadam A, Millhouse PW, Kepler CK, et al. Bone substitutes and expanders in Spine Surgery: A review of their fusion efficacies. *Int J Spine Surg* 2016;10:33.
- Sasani M, Ozer AF. Single-stage posterior corpectomy and expandable cage placement for treatment of thoracic or lumbar burst fractures. *Spine* 2009;34(1):E33–E40.

40. Koreckij TD, Gandhi SD, Park DK. Cervical Disk Arthroplasty. *J Am Acad Orthop Surg* 2019;27(3):e96–e104.
41. Leven D, Meaike J, Radcliff K, Qureshi S. Cervical disc replacement surgery: indications, technique, and technical pearls. *Curr Rev Musculoskelet Med* 2017;10(2):160–169.
42. Salzmänn SN, Plais N, Shue J, Girardi FP. Lumbar disc replacement surgery: successes and obstacles to widespread adoption. *Curr Rev Musculoskelet Med* 2017;10(2):153–159.
43. Ortiz AO, de Moura A, Johnson BA. Postsurgical Spine: Techniques, Expected Imaging Findings, and Complications. *Semin Ultrasound CT MR* 2018;39(6):630–650.
44. Weisbrod LJ, Arnold PM, Leever JD. Radiographic and CT Evaluation of Recombinant Human Bone Morphogenetic Protein-2-assisted Cervical Spinal Interbody Fusion. *Clin Spine Surg* 2019;32(2):71–79.
45. Park JB, Cho YS, Riew KD. Development of adjacent-level ossification in patients with an anterior cervical plate. *J Bone Joint Surg Am* 2005;87(3):558–563.
46. Herrera Herrera I, Moreno de la Presa R, González Gutiérrez R, Bárcena Ruiz E, García Benassi JM. Evaluation of the postoperative lumbar spine. *Radiologia (Madr)* 2013;55(1):12–23.
47. Fritz J, Lurie B, Miller TT, Potter HG. MR imaging of hip arthroplasty implants. *RadioGraphics* 2014;34(4):E106–E132.
48. Fritz J, Lurie B, Potter HG. MR Imaging of Knee Arthroplasty Implants. *RadioGraphics* 2015;35(5):1483–1501.
49. Pace N, Marinelli M, Spurio S. Technical and histologic analysis of a retrieved carbon fiber-reinforced poly-ether-ether-ketone composite alumina-bearing liner 28 months after implantation. *J Arthroplasty* 2008;23(1):151–155.
50. Lewandrowski KU, Nanson C, Calderon R. Vertebral osteolysis after posterior interbody lumbar fusion with recombinant human bone morphogenetic protein 2: a report of five cases. *Spine J* 2007;17(5):609–614.
51. Malhotra A, Kalra VB, Wu X, Grant R, Bronen RA, Abbed KM. Imaging of lumbar spinal surgery complications. *Insights Imaging* 2015;6(6):579–590.
52. Cannada LK, Scherping SC, Yoo JU, Jones PK, Emery SE. Pseudoarthrosis of the cervical spine: a comparison of radiographic diagnostic measures. *Spine* 2003;28(1):46–51.
53. Amiri AR, Fouyas IP, Cro S, Casey AT. Postoperative spinal epidural hematoma (SEH): incidence, risk factors, onset, and management. *Spine J* 2013;23(2):134–140.
54. Post MJ, Becerra JL, Madsen PW, et al. Acute spinal subdural hematoma: MR and CT findings with pathologic correlates. *AJNR Am J Neuroradiol* 1994;15(10):1895–1905.
55. Capen DA, Calderone RR, Green A. Perioperative risk factors for wound infections after lower back fusions. *Orthop Clin North Am* 1996;27(1):83–86.
56. Garrett MP, Kakarla UK, Porter RW, Sonntag VK. Formation of painful seroma and edema after the use of recombinant human bone morphogenetic protein-2 in posterolateral lumbar spine fusions. *Neurosurgery* 2010;66(6):1044–1049; discussion 1049.
57. Hawk MW, Kim KD. Review of spinal pseudomeningoceles and cerebrospinal fluid fistulas. *Neurosurg Focus* 2000;9(1):e5.
58. Luetmer PH, Schwartz KM, Eckel LJ, Hunt CH, Carter RE, Diehn FE. When should I do dynamic CT myelography? Predicting fast spinal CSF leaks in patients with spontaneous intracranial hypotension. *AJNR Am J Neuroradiol* 2012;33(4):690–694.
59. Quail A. Infections associated with spinal implants. *Int Orthop* 2012;36(2):451–456.
60. Pull ter Gunne AF, Hosman AJ, Cohen DB, et al. A methodological systematic review on surgical site infections following spinal surgery. I. Risk factors. *Spine* 2012;37(24):2017–2033.